DISCLAIMER

This report was prepared as an account of work sponsored by an agency of the United States Government. Neither the United States Government nor any agency thereof, nor any of their employees, makes any warranty, express or implied, or assumes any legal liability or responsibility for the accuracy, completeness, or usefulness of any information, apparatus, product, or process disclosed, or represents that its use would not infringe privately owned rights. Reference herein to any specific commercial product, process, or service by trade name, trademark, manufacturer, or otherwise does not necessarily constitute or imply its endorsement, recommendation, or favoring by the United States Government or any agency thereof. The views and opinions of authors expressed herein do not necessarily state or reflect those of the United States Government or any agency thereof. Reference herein to any social initiative (including but not limited to Diversity, Equity, and Inclusion (DEI); Community Benefits Plans (CBP); Justice 40; etc.) is made by the Author independent of any current requirement by the United States Government and does not constitute or imply endorsement, recommendation, or support by the United States Government or any agency thereof.

SANDIA REPORT
SAND2025-11964
Printed September 2025

Sandia National Laboratories

GADRAS-DRF Validation for Safeguards and Custom Peak Fit Enhancements

Megan R. Smith, Steve M. Horne

Prepared by
Sandia National Laboratories
Albuquerque, New Mexico
87185 and Livermore,
California 94550

Issued by Sandia National Laboratories, operated for the United States Department of Energy by National Technology & Engineering Solutions of Sandia, LLC.

NOTICE: This report was prepared as an account of work sponsored by an agency of the United States Government. Neither the United States Government, nor any agency thereof, nor any of their employees, nor any of their contractors, subcontractors, or their employees, make any warranty, express or implied, or assume any legal liability or responsibility for the accuracy, completeness, or usefulness of any information, apparatus, product, or process disclosed, or represent that its use would not infringe privately owned rights. Reference herein to any specific commercial product, process, or service by trade name, trademark, manufacturer, or otherwise, does not necessarily constitute or imply its endorsement, recommendation, or favoring by the United States Government, any agency thereof, or any of their contractors or subcontractors. The views and opinions expressed herein do not necessarily state or reflect those of the United States Government, any agency thereof, or any of their contractors.

Printed in the United States of America. This report has been reproduced directly from the best available copy.

Available to DOE and DOE contractors from
U.S. Department of Energy
Office of Scientific and Technical Information
P.O. Box 62
Oak Ridge, TN 37831

Telephone: (865) 576-8401
Facsimile: (865) 576-5728
E-Mail: reports@osti.gov
Online ordering: http://www.osti.gov/scitech

Available to the public from
U.S. Department of Commerce
National Technical Information Service
5301 Shawnee Rd
Alexandria, VA 22312

Telephone: (800) 553-6847
Facsimile: (703) 605-6900
E-Mail: orders@ntis.gov
Online order: https://classic.ntis.gov/help/order-methods/

ABSTRACT

In previous years, SGTech funded enhancements to the uranium isotopics routine in the software called Gamma Detector Response and Analysis Software-Detector Response Function (GADRAS-DRF), including the addition of peak fit customization capabilities [1][4][3]. A project was also funded that focused on implementing a peak-based model fitting routine, allowing model fitting to be performed without dependence on export-controlled radiation transport software and cross-section libraries. In FY25 significant improvements were made to the custom peak fitting interface, accompanied by several validation studies within GADRAS-DRF. These studies encompassed IsotopeID performance, distributed source analysis, isotopics validation, and activity estimation. Additionally, the peak-only model fitting option was validated using an HPGe measurement of a rotating drum with line sources.

ACKNOWLEDGEMENTS

This work was funded by the Department of Energy, National Nuclear Security Administration, Office of International Nuclear Safeguards, NA-241. Special thanks to Reymundo Rael and Alex Christensen for assisting with some experiments that took place for the analysis in this report. Michael Enghauser also provided input on the GUI workflow and used the new GUI to do a preliminary isotopic analysis.

CONTENTS

LIST OF FIGURES

LIST OF TABLES

This page left blank

ACRONYMS AND TERMS

Acronym/Term	Definition
SME	Subject Matter Expert
GADRAS	Gamma Detector Response and Analysis Software
DRF	Detector Response Function
GUI	Graphical User Interface
SNM	Special Nuclear Material
RE	Relative Efficiency
DU	Depleted uranium
HEU	Highly enriched uranium
Pu	Plutonium
U	Uranium
HPGe	High purity germanium
FY	Fiscal Year
IAEA	International Atomic Energy Agency
FWHM	Full Width at Half Maximum
ORNL	Oak Ridge National Laboratory
LLNL	Lawrence Livermore National Laboratory
BeRP	Beryllium Reflected Plutonium
CZT	Cadmium Zinc Telluride
TCS	True Coincidence Summing

1. INTRODUCTION

The GADRAS-DRF software [1] is being evaluated as a potential tool for the International Atomic Energy Agency (IAEA) to support enrichment and isotopics analysis, automated isotope identification, and large-scale modeling efforts for training machine learning algorithms. GADRAS-DRF utilizes a detector response function (DRF) to simulate the spectra produced by a radiation detector when exposed to radiation [2]. Its capabilities include characterizing detector response parameters, visualizing both measured and simulated spectra, generating realistic spectroscopic data, and analyzing spectral information. Spectral analysis features include isotope identification and estimation of source energy distributions [1]. Currently, IsotopeID, part of GADRAS-DRF, has already been licensed to the IAEA for use on their detectors.

The computed responses generated by GADRAS-DRF can be combined with measured spectra to determine the isotopic enrichment of uranium or plutonium, as demonstrated in a related NA-241 project titled "GADRAS-DRF Enhancements for Safeguards" [3]. Accurate peak fits are critical for reliable enrichment analysis and are particularly important when using the M400 detector, which exhibits skewing on the low- and high-energy sides of photopeaks, which is typical for cadmium zinc telluride (CZT) detectors. Previously a feature was added to GADRAS-DRF that allowed users to adjust these peak fits manually [4]. This document will describe the changes made to this peak fit customization capability. Additionally, algorithms of interest to the IAEA are validated here.

2. CUSTOM PEAK FITTING SOFTWARE IMPROVEMENTS

Significant improvements based on user feedback have been made to peak fit customization for use in the isotopics analysis routine within GADRAS-DRF, as well as peak-based inverse model analysis. In-depth details about both methods are described elsewhere [3]. This section will detail the changes to isotopics and peak fit customization. With the new changes, when users select "Analyze" from the Isotopics analysis page, shown below in Figure 1, a new form (Figure 3) is now shown at the same time as the isotopics results page (Figure 4). This allows users to view the peak fits in a graph as shown below in Figure 2. Note that the peak customization form will only be visible if users select a peak-based analysis method outlined in blue in Figure 1 below.

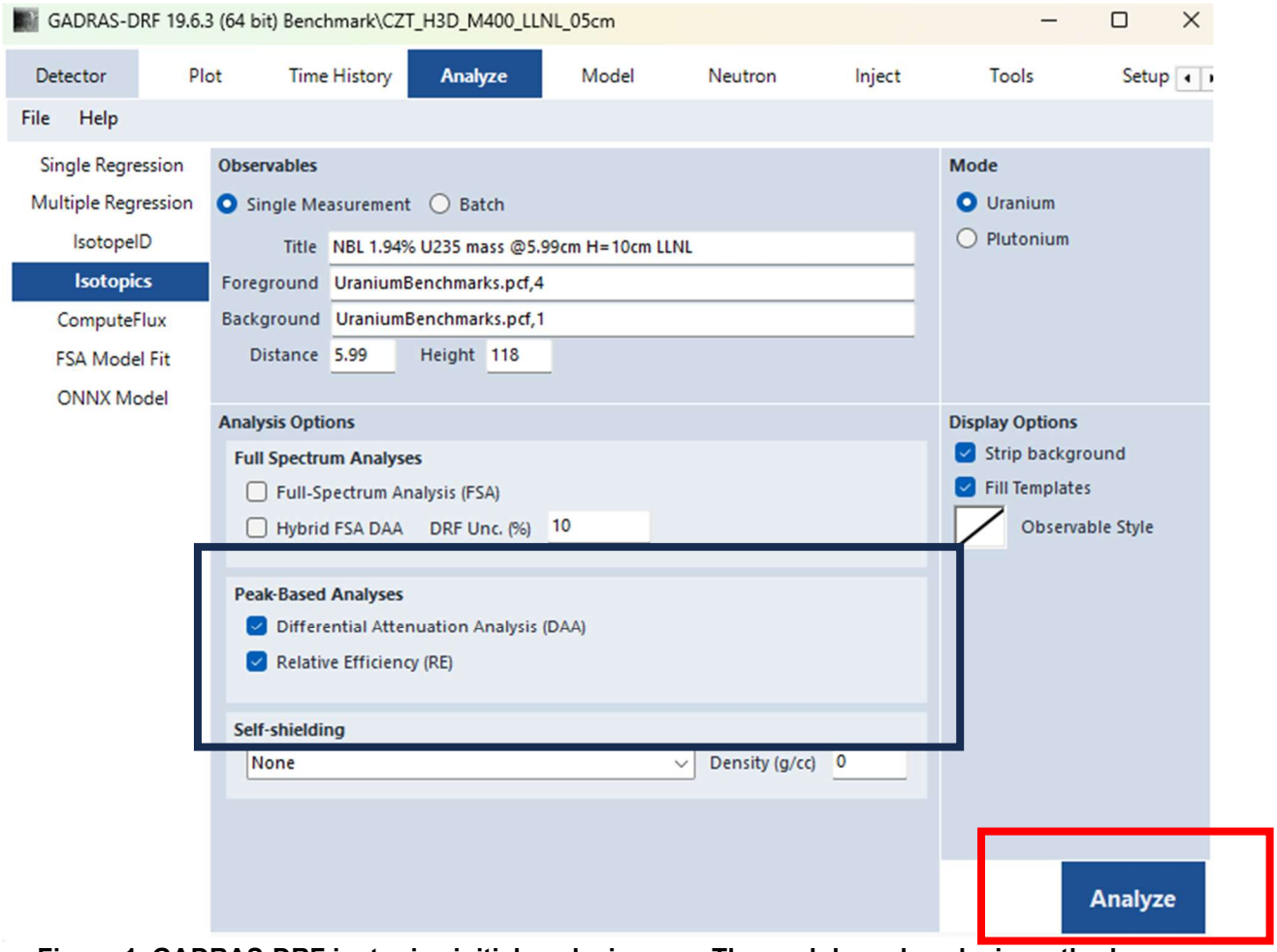

Figure 1. GADRAS-DRF isotopics initial analysis page. The peak-based analysis methods are outlined in blue and the analyze button is outlined in red.

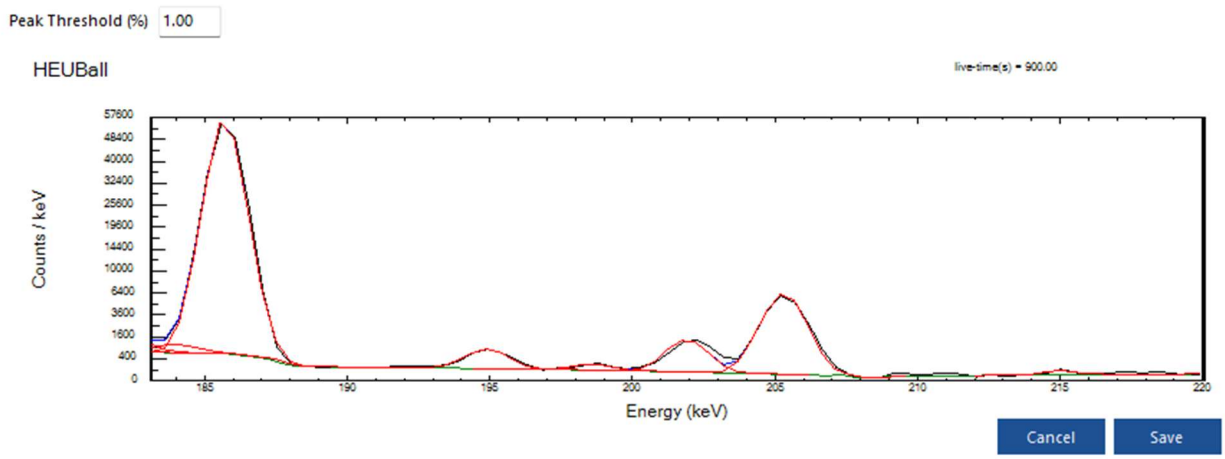

Figure 2. Gamma spectrum showing peak fits.

Figure 3. Table where users can select peaks to customize.

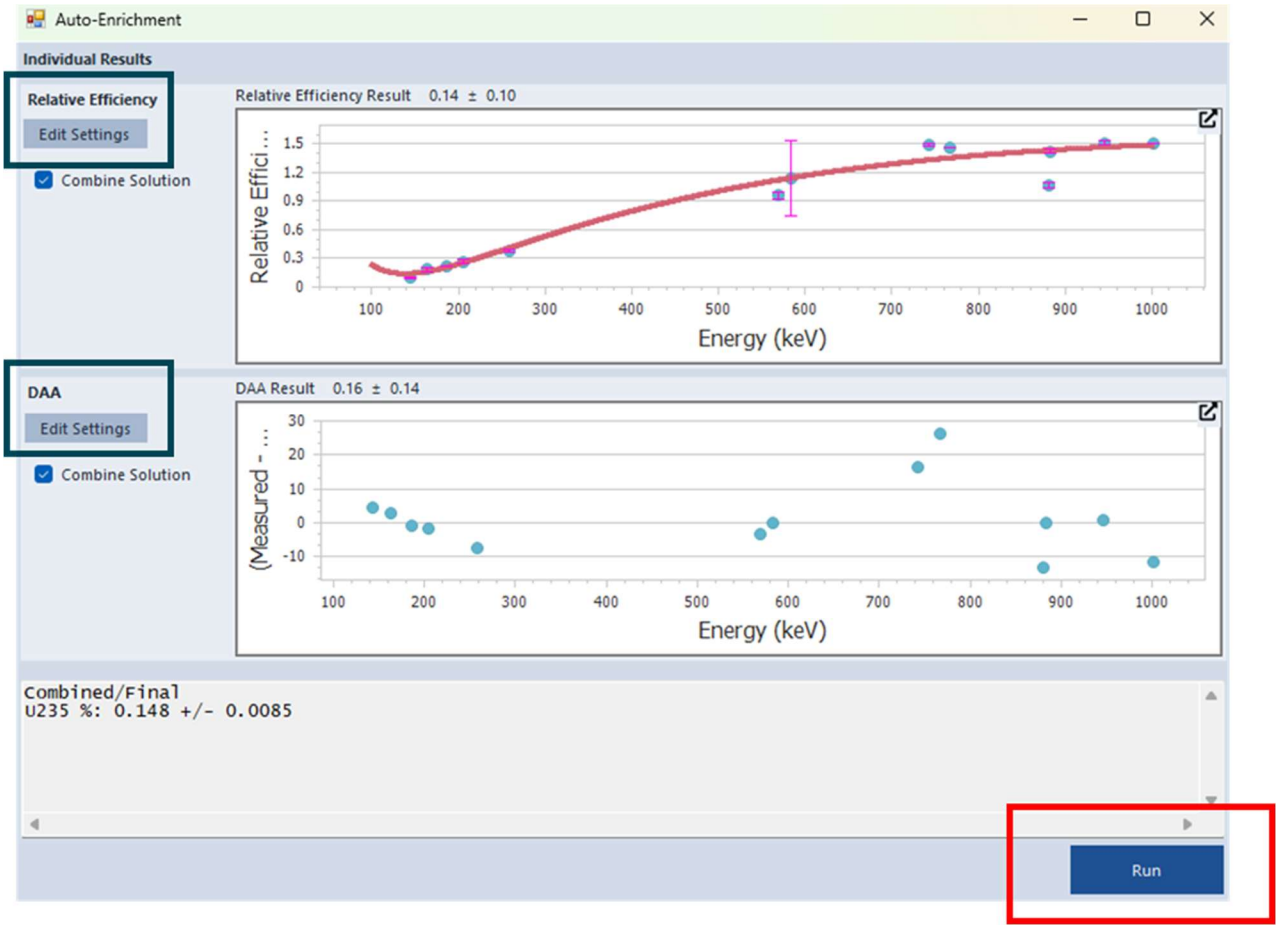

Figure 4. Isotopics results page in GADRAS-DRF.

From the table in Figure 3, users can also select which peaks are used for the different isotopics methods, namely differential attenuation analysis (DAA) and relative efficiency (RE). These options are outlined in blue. As users select and deselect peaks, or customize peaks, the isotopics form (Figure 4) will automatically update with the new results. To launch the peak fit customization form as shown below in Figure 5, users can right click on the peak in the table and select the menu option. The graph below the table shows the peak fits so users can easily see which ones could be improved. As peaks are customized, the new peak areas will automatically update the isotopic results form, and the graph below the table in Figure 3 automatically updates with the new peak fits. Additionally, on the peak customization form, users now have the ability to switch between different scales for viewing the spectrum.

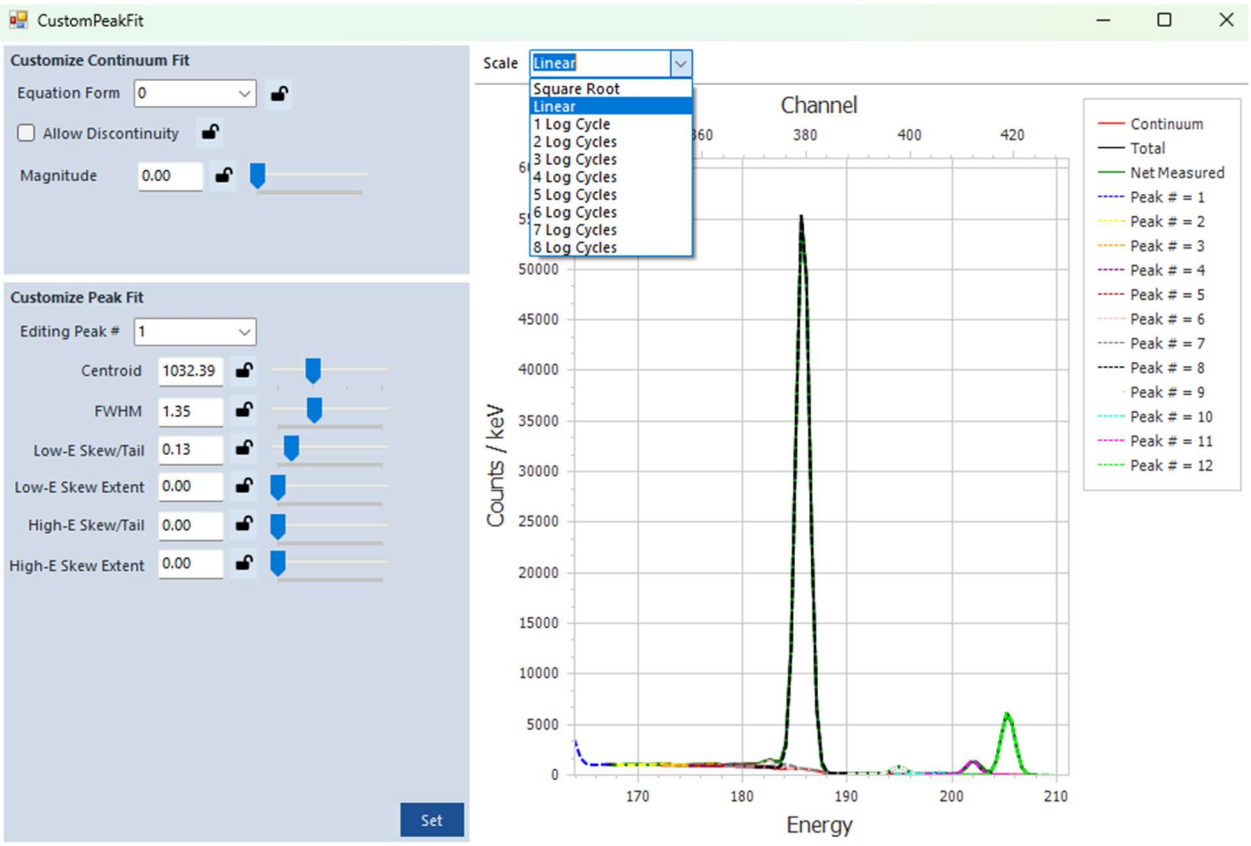

Figure 5. Peak customization form.

Additional quality of life changes were also made to peak customization. For example, if a user right clicks on a peak that was already customized, the values set by the user previously and the corrected peak shape are displayed on the peak customization form. Once users set the customization, the customized peak, along with the new peak area, is highlighted as shown below in Figure 6. Updates to the continuum fitting routine for peak customization were also made.

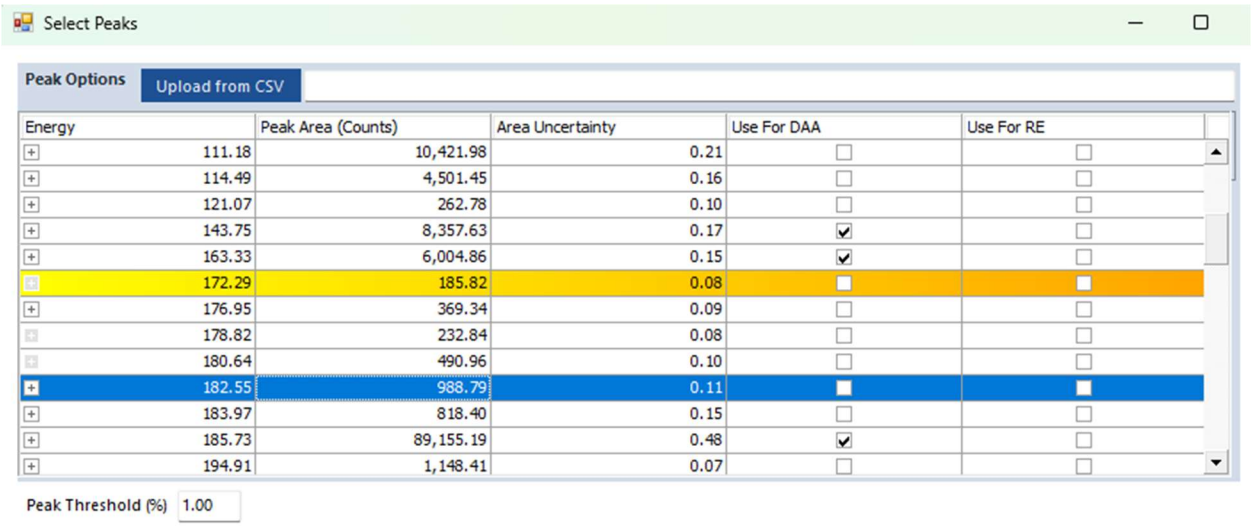

Energy	Peak Area (Counts)	Area Uncertainty	Use For DAA	Use For RE
111.18	10,421.98	0.21	☐	☐
114.49	4,501.45	0.16	☐	☐
121.07	262.78	0.10	☐	☐
143.75	8,357.63	0.17	☑	☐
163.33	6,004.86	0.15	☑	☐
172.29	185.82	0.08	☐	☐
176.95	369.34	0.09	☐	☐
178.82	232.84	0.08	☐	☐
180.64	490.96	0.10	☐	☐
182.55	988.79	0.11	☐	☐
183.97	818.40	0.15	☐	☐
185.73	89,155.19	0.48	☑	☐
194.91	1,148.41	0.07	☐	☐

Figure 6. Table of peak fits where the customized peaks are highlighted.

Users also have the ability to change the peak threshold on the peak form (Figure 3) if the threshold is set too high initially. Changing the peak threshold does not override any peak customizations provided by the user. Additionally, users have the ability to load in peak information from PeakEasy. This feature was implemented in FY24, but now isotopics updates automatically and this feature is now available for peak-only inverse model fitting. The same table in Figure 3 has been implemented when users choose to do a peak only fit for the FSA Model Fit analysis routine. As before with model fit, the table is not initially populated, but as users click on peaks in the graph displayed below the tables, the peaks are added to the table for analysis.

The last change made to isotopics was the ability to adjust the density in real-time for the DAA isotopics estimate. The density can now be adjusted two ways for DAA: selecting self-shielding and adjusting the values on that form, or by using the sliding trackbar. It is the sliding trackbar that will update the DAA results in real time. Users have the additional option of typing in a density value. Changes made will update the self-shielding form and the summary. Both options are outlined in red below in Figure 7.

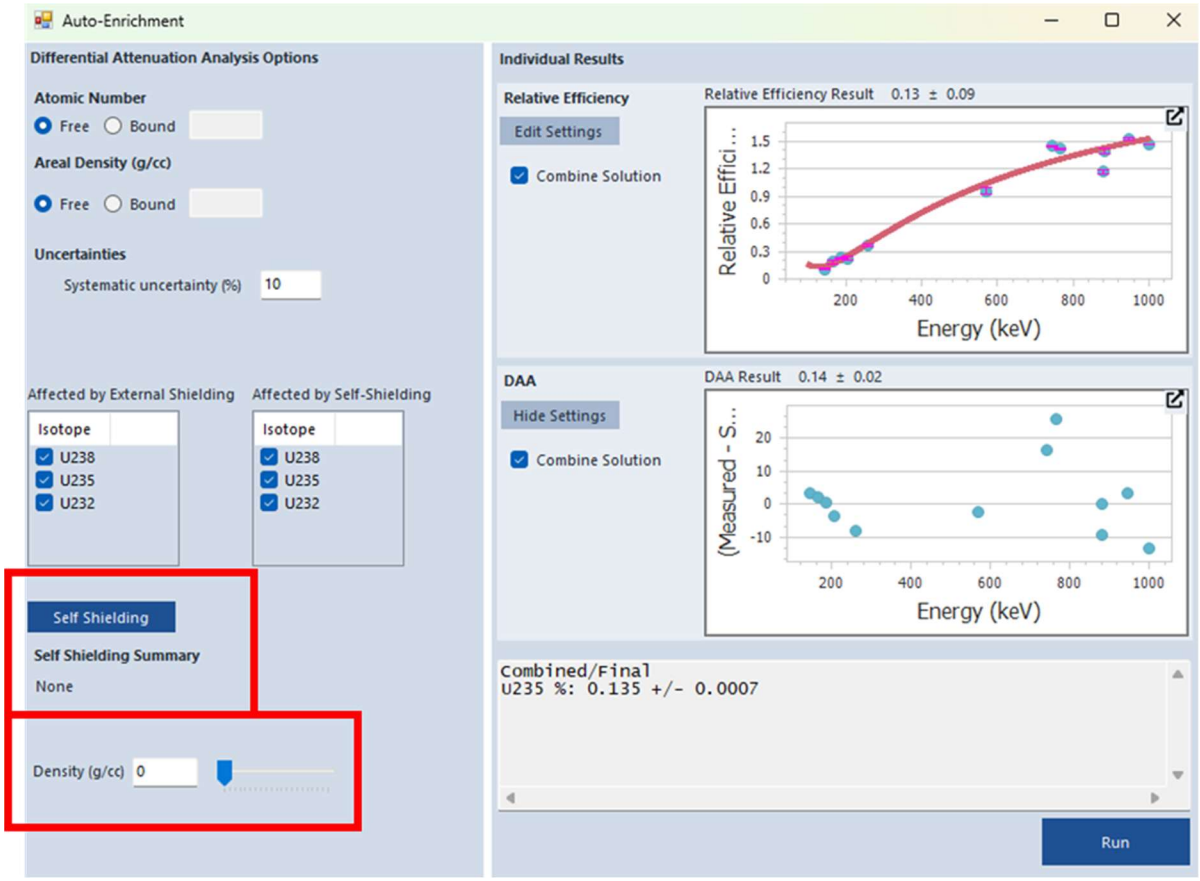

Figure 7. DAA settings where the options to adjust the density are outlined in red.

3. VALIDATION

For this study, several aspects of GADRAS-DRF were analyzed such as IsotopeID, peak only inverse model fitting, multiple regression, and isotopics. Miscellaneous items such as varying peak shapes between H3D M400 units and GADRAS-DRF's capability to account for true coincidence summing (TCS) are also discussed.

3.1. Peak Shape Comparison

The purpose of this section is to compare the peak shape of the 662 keV peak of Cs-137 between H3D M400 detectors to see if peak shapes vary between units. In FY24 the IAEA sent a measurement from one of their H3D M400 detectors that was collimated. The detector was upright with the sources placed over the face of the collimator in a clear plastic dish. The following graph in Figure 8 is a comparison of the two measurements without background subtraction:

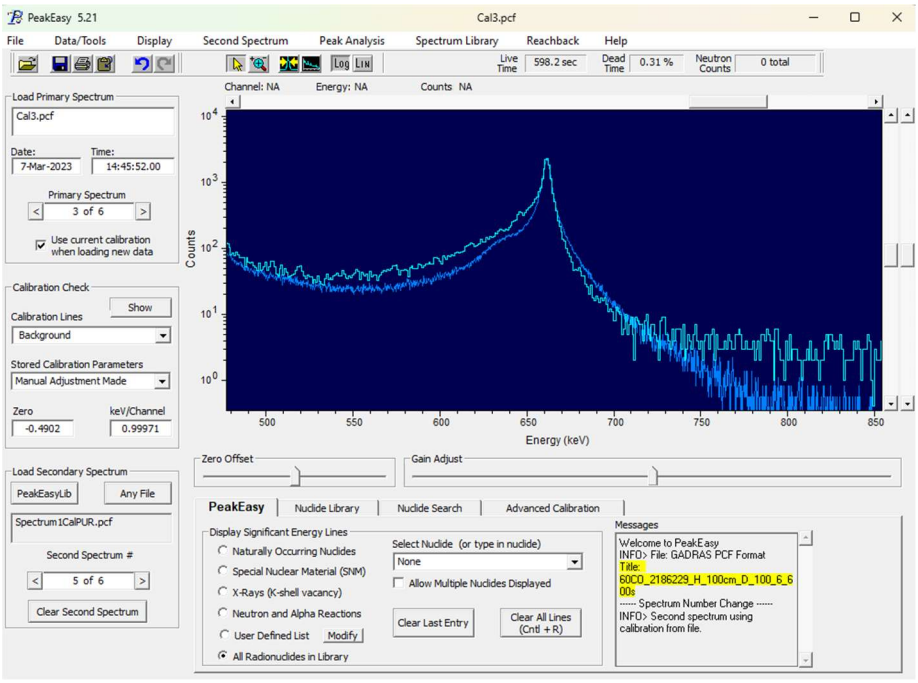

Figure 8. Cs-137 662 keV peak comparison between measurements taken by the IAEA (dark blue) and SNL (teal) without background subtraction.

The spectrum provided by the IAEA is in dark blue. There is a distinctive hump before the 662 keV peak, implying there are issues with the energy calibration in some of the pixels of that detector. Note that in the measurements taken by SNL (teal), the crystal had yet to be sent to H3D for maintenance. The result is the same with the background subtracted measurements shown below in Figure 9:

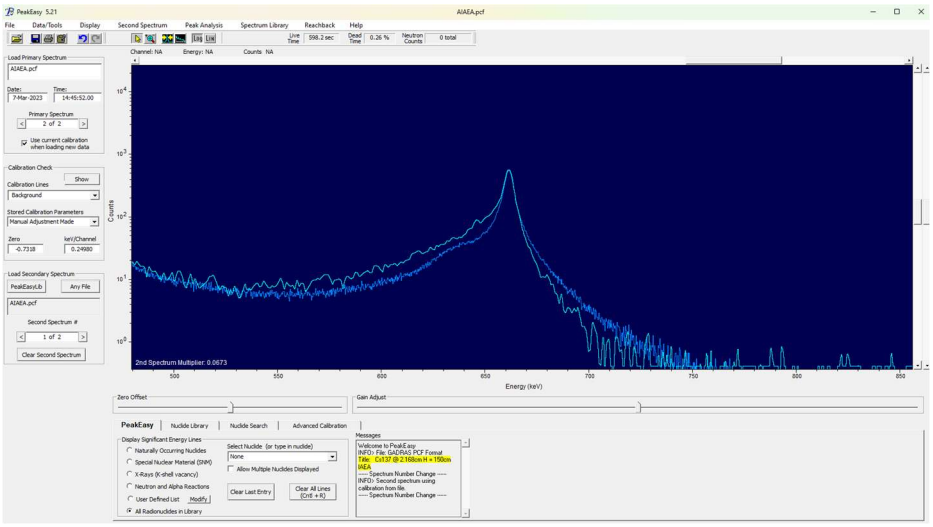

Figure 9. Cs-137 662 keV peak comparison between measurements taken by the IAEA (dark blue) and SNL (teal) with background subtraction.

Although the two measurements were taken in different configurations, the peak shape should ideally be similar. For these two detectors the peak shapes are not the same, at least within the region where skew is viewed. In Figure 10 below it looks as if the full width at tenth max matches between the two detectors.

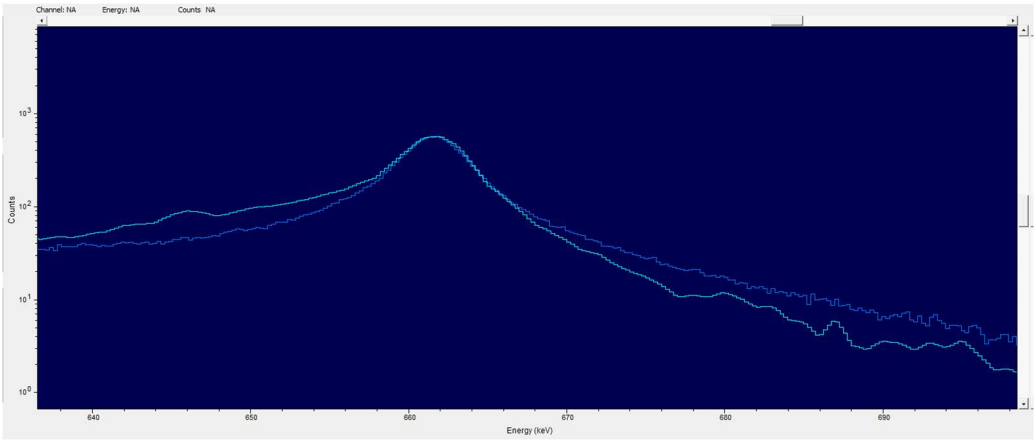

Figure 10. Zoomed in Cs-137 662 keV peak comparison between measurements taken by the IAEA (dark blue) and SNL (teal) with background subtraction.

3.2. Task 2.4 Validate IsotopeID

Various experiments were used to validate IsotopeID: rotating line sources in a uniform drum to simulate a distributed source, measurements taken at different distances than characterization measurements, and measurements using NBL uranium standards. Most measurements were done using an H3D M400 detector, while others were done using an HPGe Detective-DX100 detector.

3.2.1. Uniform Rotating Drum Measurements – HPGe

The following analysis using IsotopeID in GADRAS-DRF is meant to showcase the ID capabilities for a uniformly distributed source when the characterization was performed using point sources. The following measurements were taken using an HPGe Detective-DX100. The sources used are linear sources made of a mix of radionuclides shown in Table 1 below.

Table 1. Radionuclides used to simulate a uniform distribution in a drum with a reference day of May 1st, 2008.

Radionuclide	Activity	Source ID
Am-241	10.63 μCi	RS00287
Eu-152	5.174 μCi	
Cs-137	5.252 μCi	
Am-241	10.58 μCi	RS00288
Eu-152	5.15 μCi	
Cs-137	5.224 μCi	
Am-241	10.53 μCi	RS00289
Eu-152	5.132 μCi	
Cs-137	5.174 μCi	
Am-241	10.66 μCi	RS00290
Eu-152	5.216 μCi	
Cs-137	5.231 μCi	
Am-241	10.57 μCi	RS00291
Eu-152	5.164 μCi	
Cs-137	5.207 μCi	
Am-241	10.72 μCi	RS00292
Eu-152	5.205 μCi	
Cs-137	5.237 μCi	

The activities are uniformly distributed in an epoxy matrix with a density of 1.07 g/cc and case in a 9.53 mm tube (outer dimension) of aluminum that is 813 mm long with a wall thickness of 0.89 mm. Both ends are capped with 2mm plugs, resulting in an active length of 809 mm. The sources were placed in a drum with source locations marked 1-8 as shown in the image below. The drum shown below is filled with foam. Two other drums with different fill material were also used for measurements: One drum was filled with fiberboard and the other had wood.

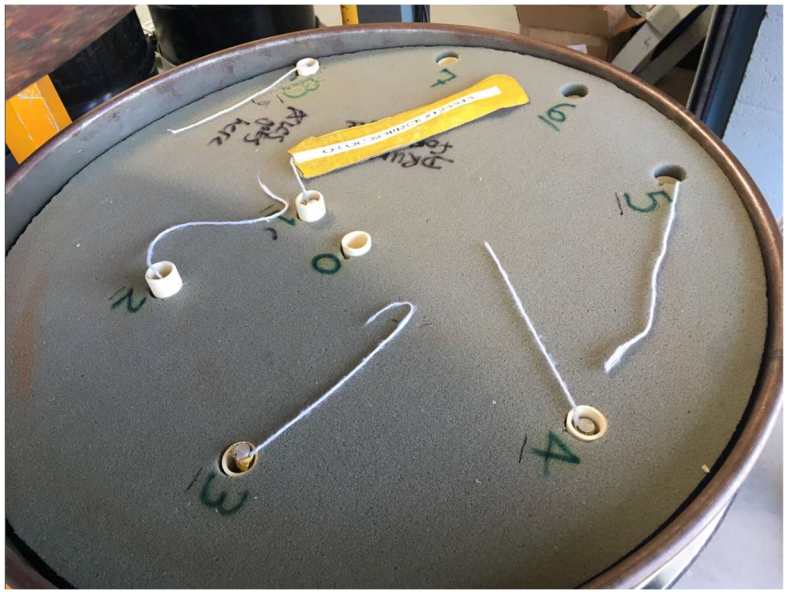

Figure 11. Placement of sources in the foam drum. The numbers are used to indicate source placement for the sources shown in Table 2. This setup is the same in the other drums.

The sources from Table 1 were placed in the various locations indicated below in Table 2 where the numbers are marked in the above figure.

Table 2. Sources and their corresponding placements in the drums.

Source	Number Location
RS-0287	1
RS-0288	2
RS-0289	3
RS-0290	4
RS-0291	5
RS-0292	8

The drum was then rotated during the measurement to make it look like a distributed source. The detector used for the drum measurements was characterized using a standard set of characterization measurements: Am-241, Cs-137, Co-60, U-232. The characterization distance was 100 cm at a height of 122 cm off the ground. For the drum measurements, the detector was 100 cm from the center of the drum. Using this detector characterization and the drum measurement, IsotopeID in GADRAS-DRF identifies the isotopes shown in Figure 12 below for the drum filled with foam.

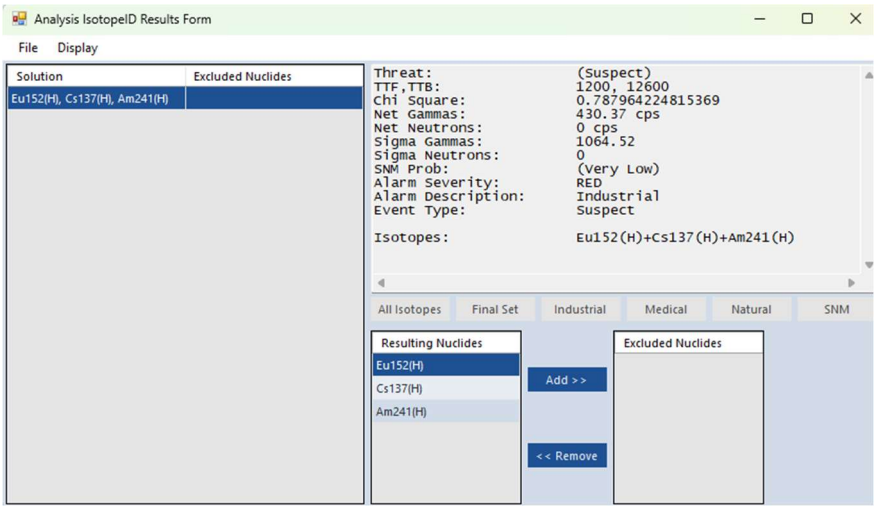

Figure 12. IsotopeID results for the uniform drum measurement where the drum was filled with foam.

As shown, IsotopeID successfully identified all sources present for a uniform source when the characterization was done using point sources. GADRAS-DRF will attempt to fill in the measured spectrum with the radionuclides identified. The radionuclide contribution to the spectrum is shown in Figure 13 where the spectrum is fully filled in, implying that all radionuclides present were identified.

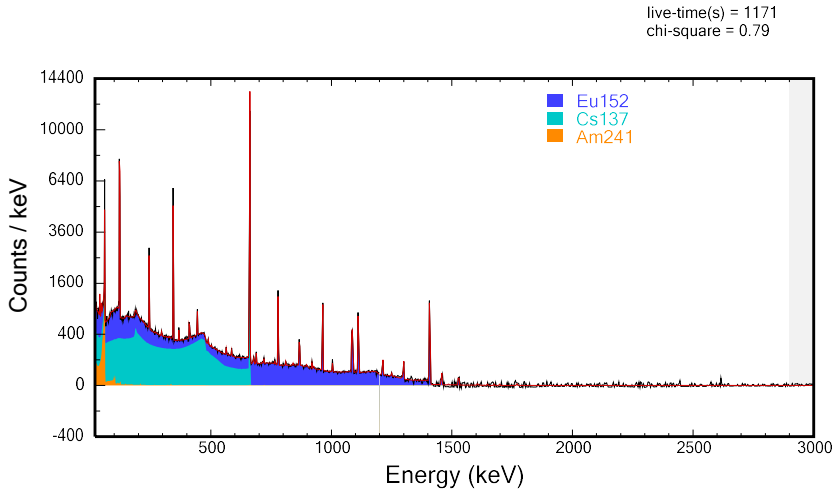

Figure 13. IsotopeID result contributions to the measured spectrum.

The following default analysis settings in Figure 14 were used for the analysis of all drums. The only settings changing from the above is the foreground measurement analyzed. The results for the remaining drum measurements are shown in Figure 15 and Figure 16.

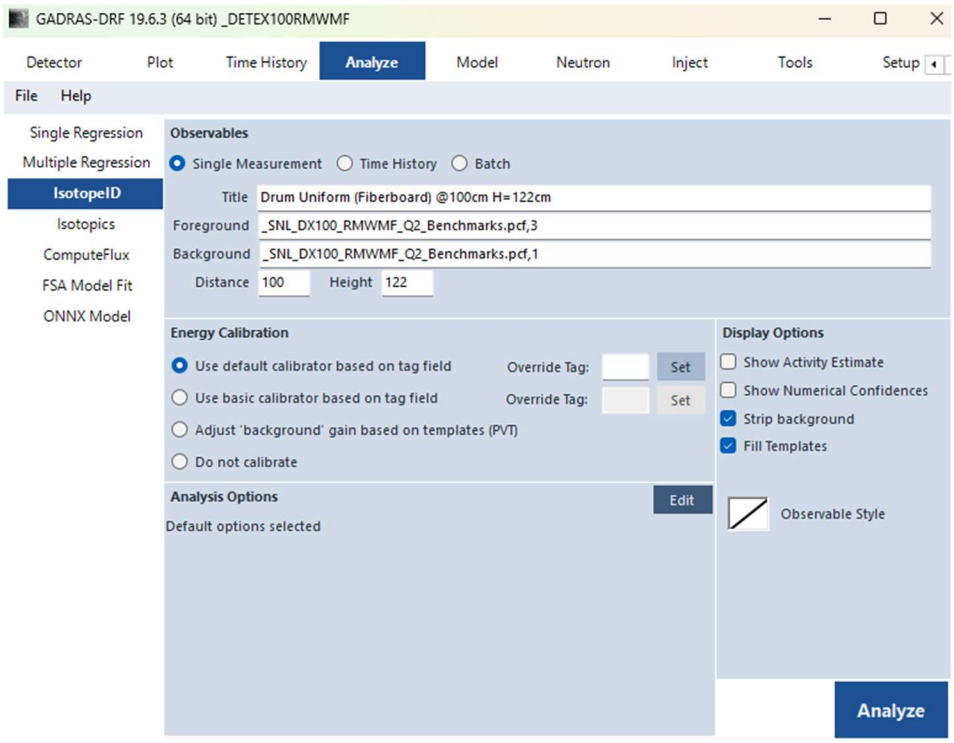

Figure 14. Default analysis settings used for the uniform drum measurements.

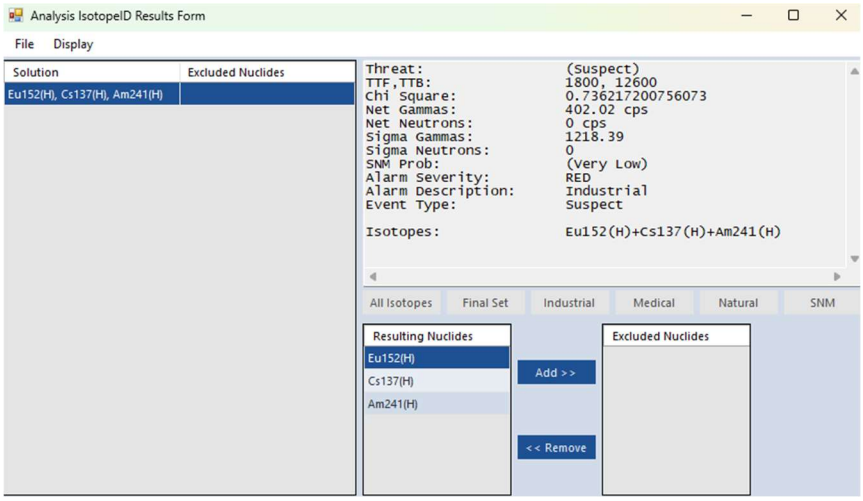

Figure 15. Results for the uniform measurement of the drum filled with fiberboard.

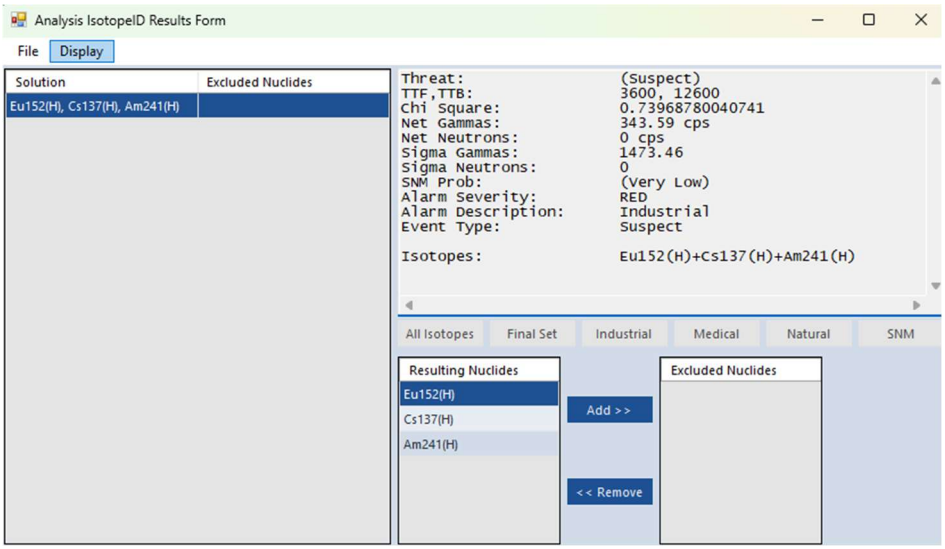

Figure 16. Results for the uniform measurement of the drum filled with wood.

Based on the results shown in this section, GADRAS-DRF can accurately identify multiple radionuclides in a spectrum for distributed sources even if the DRF was generated using a set of point sources. For this measurement with an HPGe, the standard sources were used for calibration: Co-60, Cs-137, U-232, Ba-133, and Am-241.

3.2.2. Uniform Rotating Drum Measurements – M400

The same measurements as above were repeated on June 18th 2025 using H3D's M400 detector. The same line sources from Section 3.2.1 Table 1 were used with the drum filled with fiberboard. The orientation of the line sources was also the same as shown in Figure 11. The measurements were done with the drum rotating overnight for a background and for several hours for a foreground measurement. The foreground measurement was done with the detector placed 25 cm from the outer skin of the drum. The center of the detector was 122 cm off the ground, which is at the centerline of the rotating drum. For analysis, the 25 cm DRF is used. The measurement setup is shown below in Figure 17.

Figure 17. Fiberboard rotating drum measurement setup using the H3D M400 at a distance of 25 cm from the skin of the drum.

The M400 measurement with the fiberboard drum was also analyzed with IsotopeID just like in Section 3.2.1 and the results are below from Figure 18 to Figure 20 where the last figure shows the

settings for IsotopeID used for the analysis and Figure 19 shows the spectral decomposition of the contributing radionuclides to the measured spectrum. For the M400 IsotopeID accurately detects all radionuclides present for a distributed source.

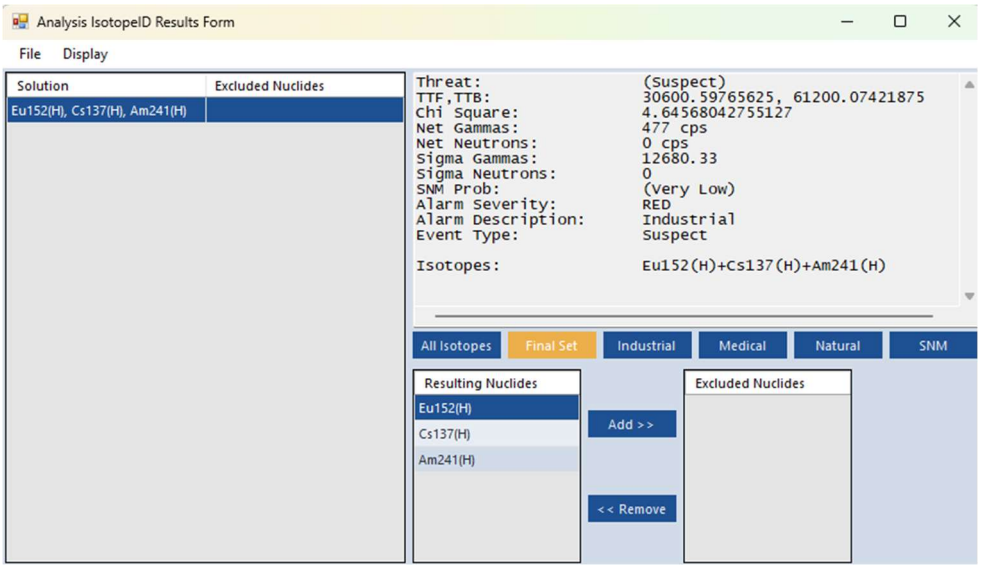

Figure 18. IsotopeID results for the fiberboard rotating drum measured using an H3D M400 detector.

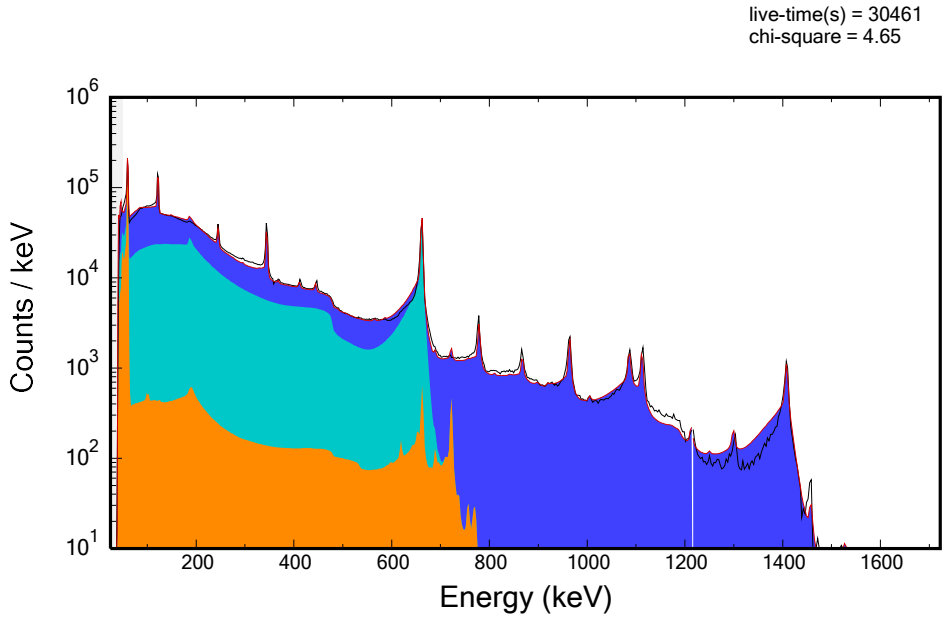

Figure 19. Spectral contribution of each isotope identified using IsotopeID.

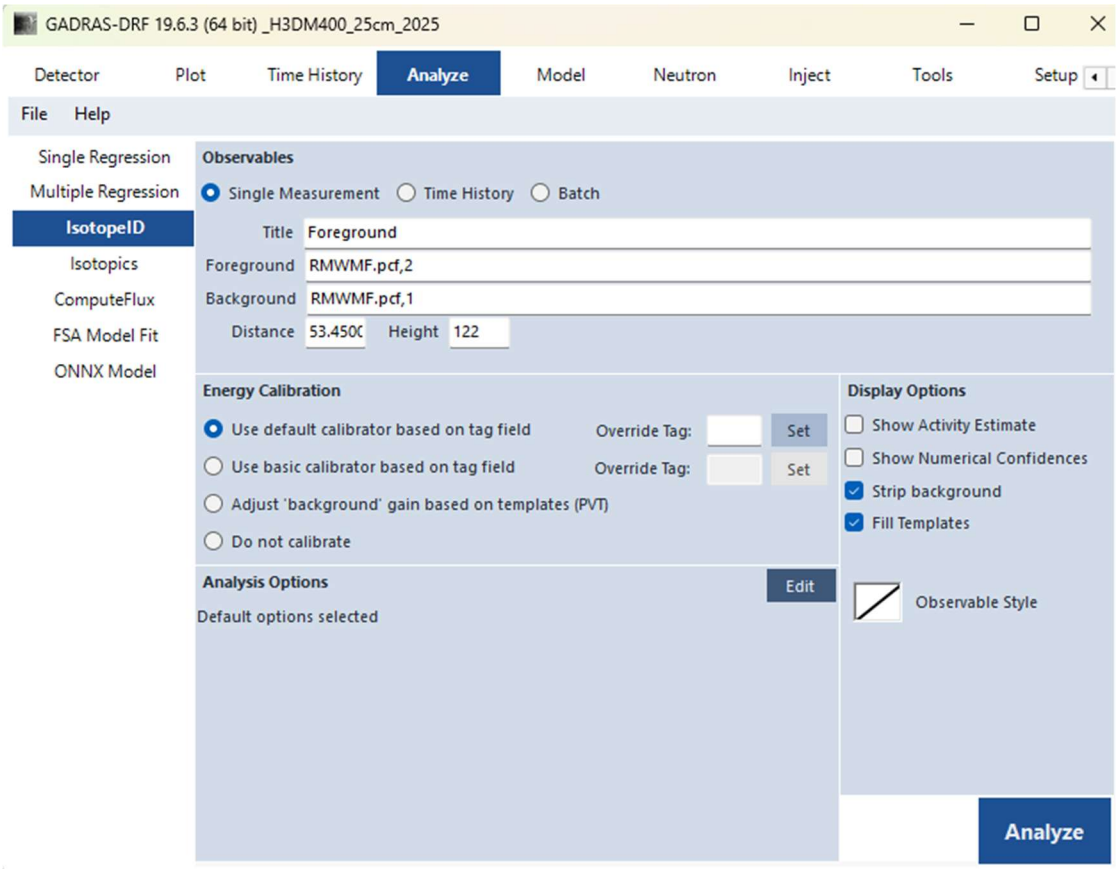

Figure 20. GADRAS-DRF settings for IsotopeID on the rotating drum measurement.

3.2.3. IsotopeID validation for measurements at various distances

The following measurements were taken with H3D's M400 CZT detector. As stated previously, a characterization was done for the detector using standard point sources placed 100 cm away from the detector at a height of 100 cm off the floor (both the source and the detector). Additionally, measurements were taken at various distances from the detector, and further measurement details can be found elsewhere [5]. Batch IsotopeID was used on these measurements and the results are shown in Table 3.

Table 3. IsotopeID results for measurements taken at various distances and a height of 100 cm.

Source	Activity	Distance (cm)	IsotopeID Result
Cs-137	120.99 μCi	10	Cs137(H)
Cs-137	120.99 μCi	20.2	Cs137(H)
Cs-137	120.99 μCi	50.3	Cs137(H)
Cs-137	120.99 μCi	199	Cs137(H)
Co-60	110.14 μCi	10	Co60(H)
Co-60	110.14 μCi	20.2	Co60(H
Co-60	110.14 μCi	50.3	Co60(H)
Co-60	110.14 μCi	199	Co60(H)

Ba-133	82.65 μCi	10	Ba133(H)
Ba-133	82.65 μCi	20.2	Ba133(H)
Ba-133	82.65 μCi	50.3	Ba133(H)
Ba-133	82.65 μCi	199	Ba133(H)

3.2.4. IsotopeID validation using NBL standards CZT H3D M400

The following measurements were also taken using H3D's M400 CZT. A set of measurements were done by LLNL using NBL standards. More details of the experimental setup can be found elsewhere, and a photo of the setup is shown below in Figure 21 [10].

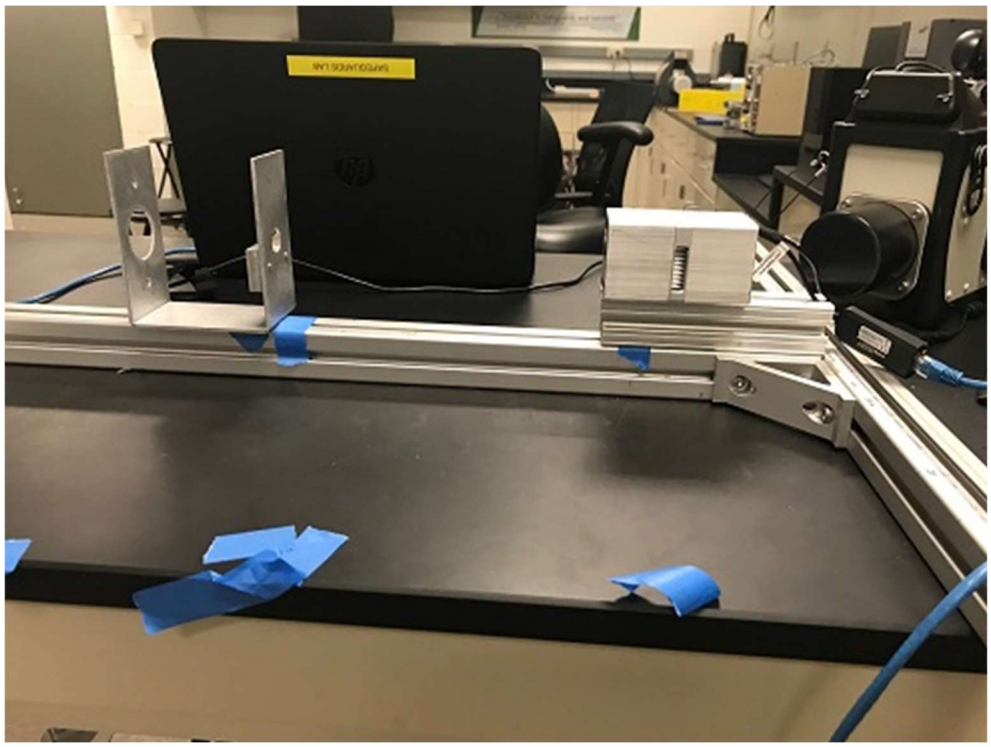

Figure 21. LLNL experimental setup for measuring NBL standards using an H3D M400 [10].

The characterization measurements were done using point sources U-232, Am-241, Cs-137, and Co-60. The calibration measurements were done at the same distances as the measurements. The calibration measurements below were taken at LLNL. The U_3O_8 standards used for IsotopeID are shown below in Table 4.

Table 4. Uranium NBL standards measured at LLNL [8][9].

Detector	Source	U-235 Weight %	Source Shielding	Distance (cm)
Unshielded	NBL (SRM 969)	0.31	Unshielded	5 & 25
Unshielded	NBL (SRM 969)	0.71	Unshielded	5 & 25
Unshielded	NBL (SRM 969)	1.94	Unshielded	5 & 25
Unshielded	NBL (SRM 969)	2.95	Unshielded	5 & 25
Unshielded	NBL (SRM 969)	4.46	Unshielded	5 & 25
Unshielded	NBL (CRM 146)	20.11	Unshielded	5 & 25
Unshielded	NBL (CRM 146)	52.49	Unshielded	5 & 25
Unshielded	NBL (CRM 146)	93.17	Unshielded	5 & 25

The standards were ran through IsotopeID in GADRAS using the batch functionality and the results are in Table 5 below.

Table 5. NBL standard measurement IsotopeID results. Distance measured was 5.99 cm and the height was 8.54 cm from the table, which was 110 cm off the floor.

Measurement	Date	Isotopes	Distance (cm)
NBL 0.31% U235 mass	Apr-10-2021	U238(H)+U235(H)	5.99
NBL 0.71% U235 mass	Apr-09-2021	U238(H)+U235(H)	5.99
NBL 1.94% U235 mass	Apr-09-2021	U235(H)+U238(H)	5.99
NBL 2.95% U235 mass	Apr-09-2021	U238(H)+U235(H	5.99
NBL 4.46% U235 mass	Apr-09-2021	U238(H)+U235(H)	5.99
NBL 20.11% U235 mass	Apr-09-2021	U235(H)+U238(H)+U232(H)	5.99
NBL 52.49% U235 mass	Apr-09-2021	U235(H)+U238(H)	5.99
NBL 93.17% U235 mass	Apr-09-2021	U235(H)+U232(H)	5.99

There was also another measurement available from LLNL where the measurements were performed at a distance of 25.99 cm from the source. These were also run through IsotopeID and the results are below.

Table 6. NBL standard measurement IsotopeID results. Distance measured was 25.99 cm and the height was 8.54 cm from the table, which was 110 cm off the floor.

Measurement	Date	Isotopes	Distance (cm)
NBL 0.31% U235 mass	Aug-28-2020	U238(H)+U235(H)	25.99
NBL 0.71% U235 mass	Aug-28-2020	U238(H)+U235(H)	25.99
NBL 1.94% U235 mass	Aug-28-2020	U238(H)+U235(H)	25.99
NBL 2.95% U235 mass	Aug-28-2020	U238(H)+U235(H)	25.99
NBL 4.46% U235 mass	Aug-28-2020	U238(H)+U235(H)	25.99
NBL 20.11% U235 mass	Aug-28-2020	U235(H)+U238(H)	25.99
NBL 52.49% U235 mass	Aug-29-2020	U235(H)+U238(H)	25.99
NBL 93.17% U235 mass	Aug-29-2020	U235(H)+U232(H)	25.99

In every measurement, U-235 was correctly identified as being present by the IsotopeID algorithm. For the 93.17% U-235 enrichment measurement, it is not uncommon to see U-232 identified as well since U-232 is a common contaminant in US created HEU. For the HEU samples (93.17% U-235) in both of the above tables, the signature from the U-238 is weak compared to the other isotopes found, so it was not identified.

3.3. Task 2.5 Isotopic Validation

Previously, subject matter expert (SME) options were added to the isotopic estimation tool in GADRAS-DRF, and the option to customize the peak fits were also added [3][4]. The purpose of this study is to use the isotopic estimation routines both with and without SME input using measurements taken by LLNL on NBL standards [8][9] to validate the isotopic estimations at various enrichments.

3.3.1. LLNL NBL Standard Measurements

The same validation standards from Table 4 in Section 3.2.4 were also used for Isotopics validation. The batch option for isotopics in GADRAS-DRF was used for the analysis and no other changes were made to the analysis results beyond the initial isotopics estimate. The densities used for the self-shielding option in GADRAS-DRF are below in Table 7, and the initial results without SME input are shown in Table 8.

Table 7. Densities of the various NBL standards used for analysis.

Measurement	Density (g/cc)
NBL (SRM 969) 0.31% U235 mass	2.50
NBL (SRM 969) 0.71% U235 mass	2.50
NBL (SRM 969) 1.94% U235 mass	2.50
NBL (SRM 969) 2.95% U235 mass	2.50
NBL (SRM 969) 4.46% U235 mass	3.29
NBL (CRM 146) 20.11% U235 mass	3.78
NBL (CRM 146) 52.49% U235 mass	3.78
NBL 93.17% U235 mass	3.78

Table 8. Isotopic analysis results for various methods RE, DAA, FSA, Hybrid, and the combined solution for various enrichments of NBL standards.

Measurement	Distance (cm)	RE	DAA	FSA	Hybrid	Combined
NBL 0.31% U235 mass	5.99	0.24 +/-0.06	0.20 +/-0.07	0.39 +/-0.18	0.34 +/- 0.01	0.33 +/-0.01
NBL 0.71% U235 mass	5.99	1.14 +/- 0.26	0.88 +/- 0.34	0.94 +/- 1.03	0.83 +/- 0.02	0.83 +/-0.11
NBL 1.94% U235 mass	5.99	1.80 +/- 0.32	1.66 +/- 0.51	2.47 +/- 0.15	2.15 +/- 0.32	2.276 +/- 0.16
NBL 2.95% U235 mass	5.99	2.49 +/- 0.77	3.61 +/- 1.4	3.80 +/- 2.28	3.34 +/- 0.52	3.14 +/- 0.24
NBL 4.46% U235 mass	5.99	4.06 +/- 0.66	4.32 +/- 1.42	6.28 +/- 7.81	5.25 +/- 1.25	4.34 +/- 0.27
NBL 20.11% U235 mass	5.99	38.33 +/- 15.53	13.11 +/- 1.53	25.72 +/- 2.12	24.01 +/- 14.11	17.82 +/- 3.49
NBL 52.49% U235 mass	5.99	65.99 +/- 13.24	37.18 +/- 5.04	60.33 +/- 3.12	57.99 +/- 11.85	54.53 +/- 5.90
NBL 93.17% U235 mass	5.99	91.84 +/-17.63	87.88 +/- 5.66	92.03 +/- 22.68	94.35 +/- 0.61	94.27 +/- 0.40

The above table shows that even without SME input, the initial default settings for the isotopics algorithms can already closely estimate the U235 enrichment when looking at the combined result column. Below in Table 9 is the solution obtained with SME input that the isotopics UI allows users to make.

Table 9. Isotopic analysis results for various methods RE, DAA, FSA, Hybrid, and the combined solution for various enrichments of NBL standards with SME input.

Measurement	Distance (cm)	RE	DAA	FSA	Hybrid	Combined
NBL 0.31% U235 mass	5.99	0.24 +/-0.04	0.21 +/- 0.07	0.41 +/- 0.06	0.33 +/- 0.01	0.33 +/- 0.01
NBL 0.71% U235 mass	5.99	0.84 +/- 0.16	0.83 +/- 0.3	0.94 +/- 0.77	0.83 +/- 0.02	0.83 +/- 0.002
NBL 1.94% U235 mass	5.99	1.77 +/- 0.27	1.53 +/- 0.43	2.47 +/- 0.15	2.15 +/- 0.32	2.22 +/- 0.19
NBL 2.95% U235 mass	5.99	2.41 +/- 0.82	3.17 +/- 1.11	3.80 +/- 2.28	3.34 +/- 0.52	3.11 +/- 0.24
NBL 4.46% U235 mass	5.99	4.06 +/- 0.66	4.32 +/- 1.42	6.28 +/- 7.81	5.25 +/- 1.25	4.34 +/- 0.27
NBL 20.11% U235 mass	5.99	20.27 +/- 9.13	13.05 +/- 2.23	25.72 +/- 2.12	24.01 +/- 14.11	19.76 +/- 3.6
NBL 52.49% U235 mass	5.99	59.74 +/- 11.69	34.29 +/- 4.80	60.33 +/- 3.12	57.99 +/- 11.85	53.15 +/- 6.64
NBL 93.17% U235 mass	5.99	91.84 +/- 17.63	87.88 +/- 5.66	92.03 +/- 22.68	94.35 +/- 0.61	94.27 +/- 0.40

Many results from the initial estimate were very close to the correct answer, so there was little room for improvement. To achieve better results, peaks that did not lie along the relative efficiency curve were excluded from the fit, and custom peak fitting was used to fit the peak areas better where needed. Special attention was paid to the 185 keV and 1001 keV peak fits. Based on DAA values, certain peaks were chosen to be excluded from the DAA estimate if the DAA values were large in magnitude.

3.3.2. Isotopic Validation BeRP Ball

GADRAS-DRF also has the ability to estimate plutonium enrichment by reporting the Pu-240 percentage. For Pu-240 isotopic estimation, only the full spectrum analysis methods are available and not the peak based methods. This is due to the peak interference between various isotopes in plutonium and the lack of peaks across the energy region. For this analysis, the BeRP (Beryllium Reflected Plutonium) ball is used to validate plutonium isotopics [11]. These measurements were taken with a 140% HPGe detector with a bismuth collimator. The analysis setup is shown below in Figure 22 and the initial results are shown in Figure 23. For self-shielding, the density of Pu alpha phase metal was used, which is 19.65 g/cc as a default in GADRAS-DRF. The combined solution from the FSA and Hybrid analysis methods gives an isotopic estimate of 5.29% +/- 0.002% Pu-240, and the ground truth for the BeRP ball is reported as 5.95% +-/ 0.01%. This is without SME input. As shown in Figure 23, there is currently an error in the uncertainty estimates for plutonium isotopics using the FSA method. This will be fixed prior to the next release of GADRAS-DRF. Improvements were made this FY for uranium isotopic uncertainty estimates, and similar changes need to be made for the plutonium isotopics.

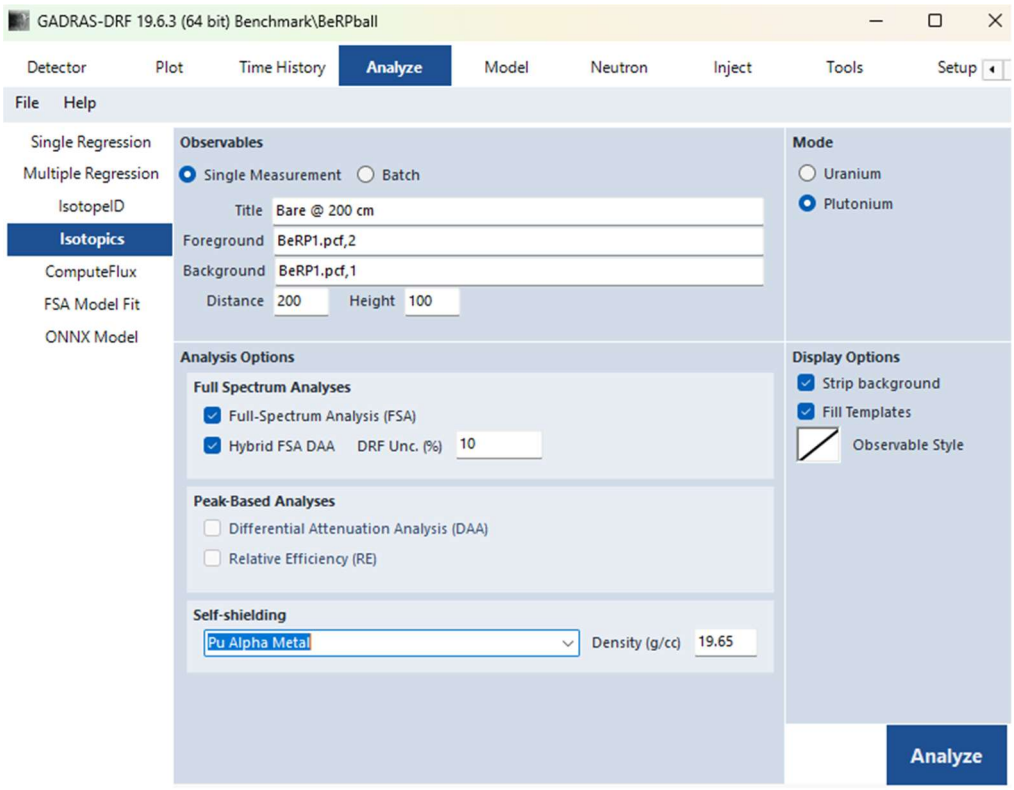

Figure 22. Analysis setup for determining Pu isotopics in the BeRP ball.

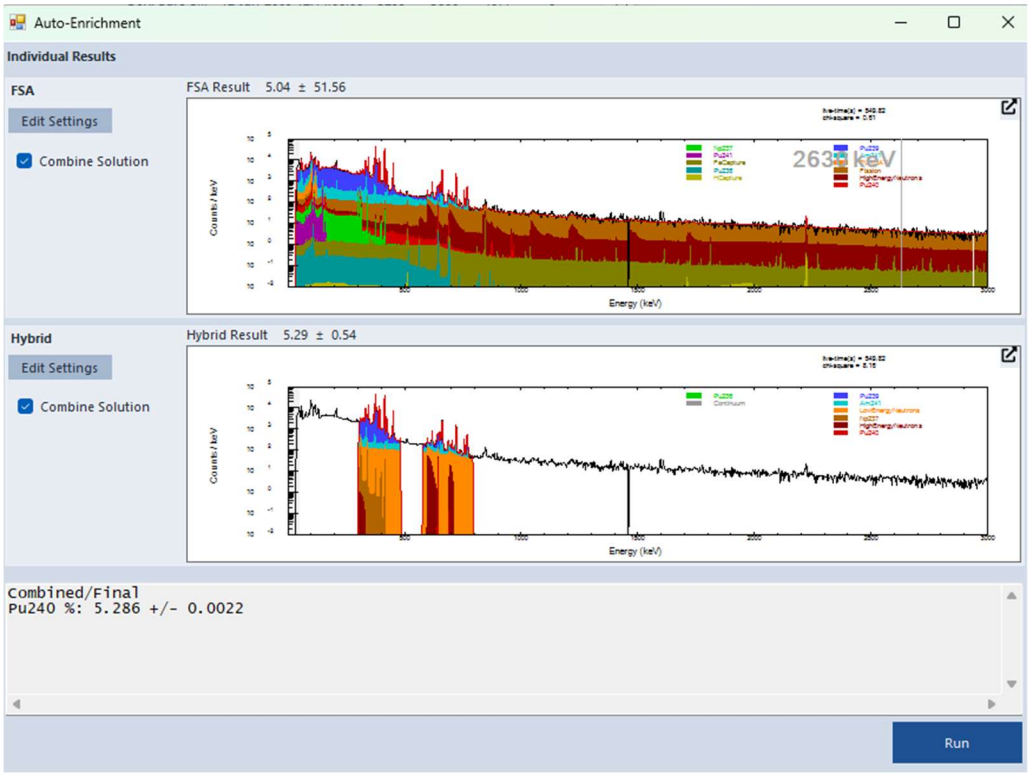

Figure 23. GADRAS-DRF Pu isotopic results for the BeRP ball.

3.4. Task 2.6 Validating Activity Estimates – H3D M400

The purpose of this section is to validate the activities estimated by GADRAS-DRF using regression. Specifically, this section looks at the activity estimates of Eu-152 measured at different distances than what the detector was characterized at. Eu-152 was also not used as a calibration source when calibrating the detector in GADRAS-DRF. H3D M400 measurements were taken at various distances. A set of calibration measurements were used to generate a DRF at 25 cm and 5 cm. It should be noted that for all DRFs generated for the H3D M400, only spectrum type 1 is used throughout this report. This is because spectrum type 2 and 3 sums and processes the data in a unique way that goes beyond the current capabilities in GADRAS. Button sources of varying strengths were used for the measurements. The sources were chosen so that the full energy range of the detector can be calibrated, and the strengths were chosen to minimize dead time while optimizing count times. Each DRF is then used to estimate the activity of Eu-152 sources that are also measured at various distances.

This section also looks at activity estimates of line sources in a rotating drum. The purpose of this was to try and simulate a distributed source in the drum. Because of this configuration and the assumptions made, this is not a good validation study for the activity estimates, but the results are presented here anyway. For multiple regression, a point source is assumed for the source geometry so multiple regression is not an ideal candidate for this situation since the source was more like a distributed source. Analysis was done for measurements taken with both an HPGe and an M400 detector.

3.4.1. H3D M400 DRF at 25cm

The activities of the sources in Table 10 are the source activities on the measurement date along with the source height and distance. The height represents both the center of the detector and source. Photos of the characterization setup can be found below in Figure 24. The characterization results using the sources in the below table are all shown in Figure 25.

Table 10. Sources used for calibration measurements for generating a DRF at 25 cm.

Source	Activity (μC)	Distance (cm)	Height (cm)	Date
Am-241	104.74	25	101.8	04/01/2025
Co-60	42.27	25	101.8	04/01/2025
Ba-133	72.12	25	101.8	04/01/2025
Cs-137	115.40	25	101.8	04/01/2025
U-232	84.74	25	101.8	04/01/2025

Figure 24. Measurement setup for M400 DRF generation at 25 cm.

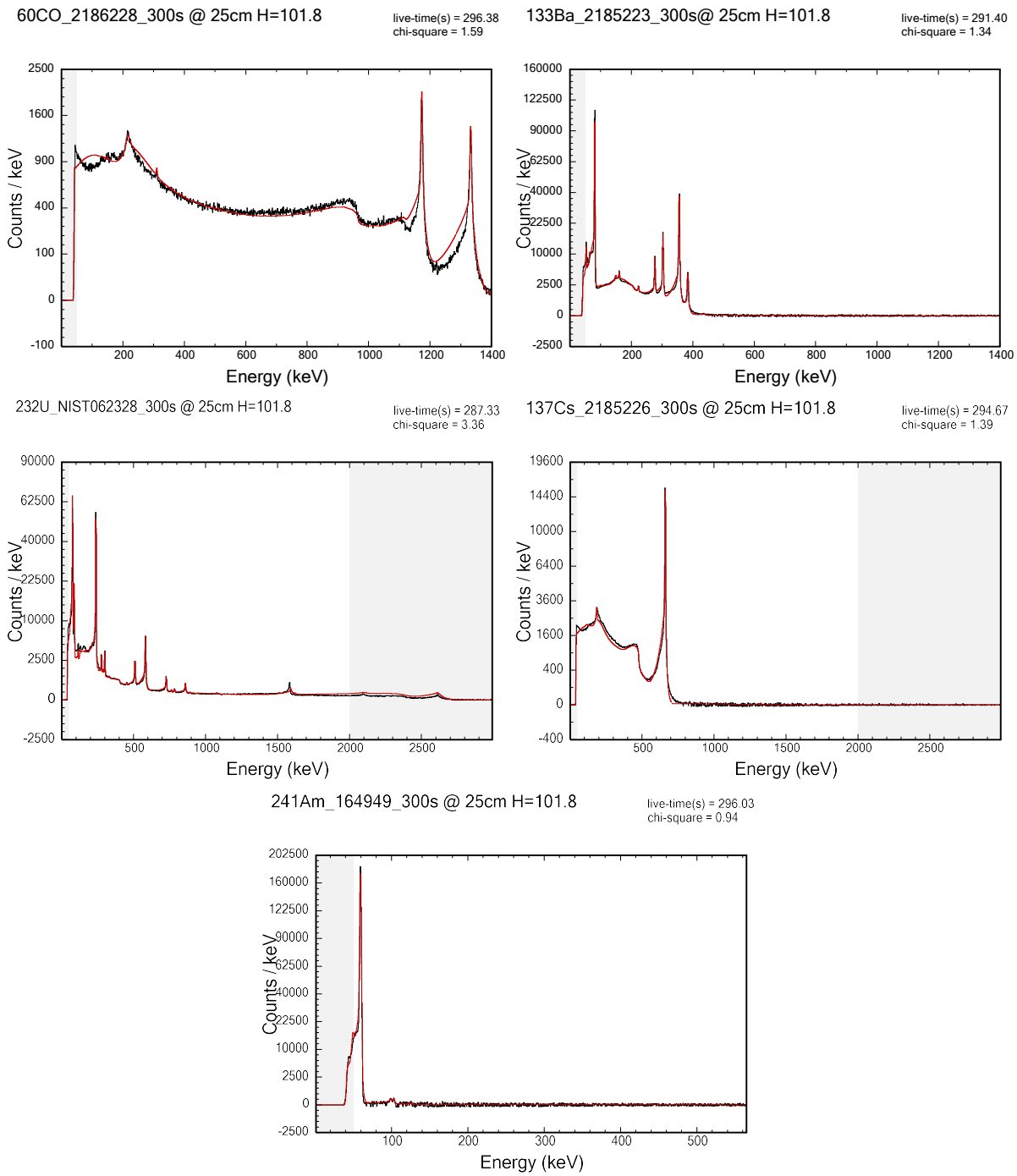

Figure 25. Characterization of the M400 DRF at 25 cm for sources listed. The simulated spectra are red, and the measured spectra are black.

The characterization is then used to estimate the activities for the Eu-152 source measured at various distances as shown below Table 11. This table has the Eu-152 distance from the source, the estimated activity using single regression in GADRAS-DRF, and the ground truth activity. The single regression settings used in GADRAS-DRF for the analysis are shown below in Figure 26. For the settings, since it is known that no known shielding is present around the source, the aerial

density for shielding was constrained to 0. Any attenuation from air between the source and the detector is already accounted for on the detector page via the distance parameter.

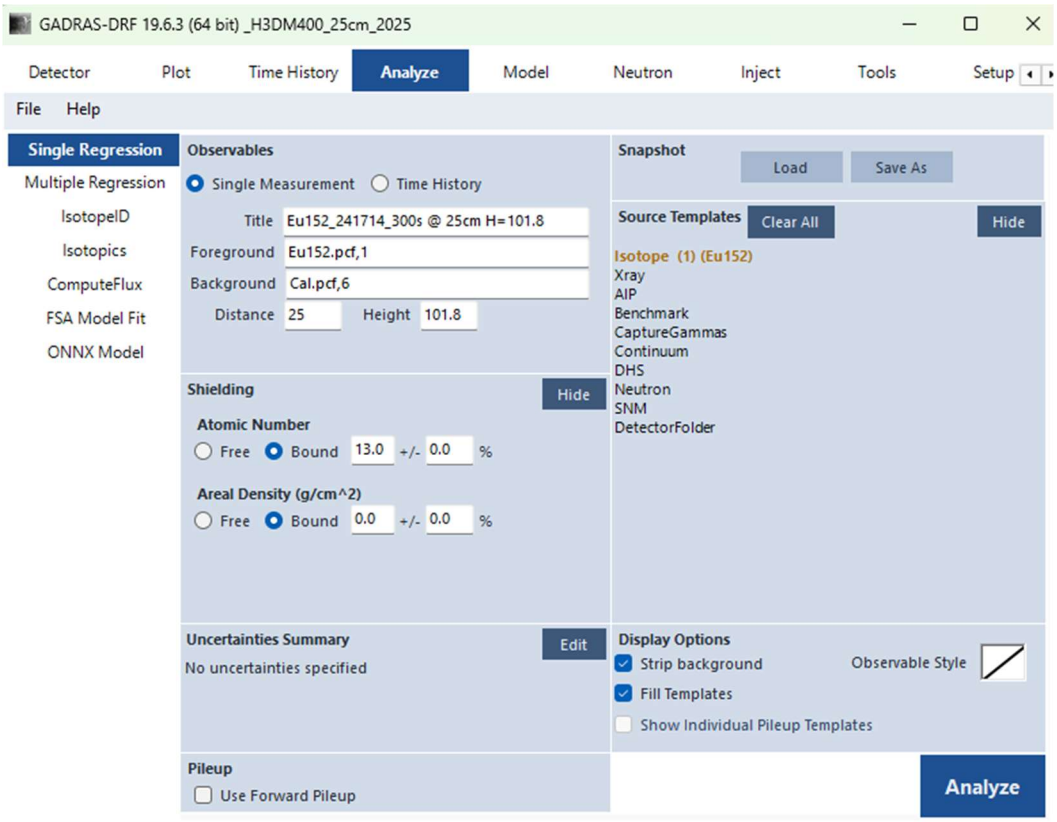

Figure 26. GADRAS-DRF analysis settings for determining Eu-152 activity using measured data.

Table 11. Eu-152 distances, ground truth activity, and estimated activity.

Source	Activity	Distance (cm)	Estimated Activity
Eu-152	48.69 μCi	25	48.56 +/- 0.13 μCi
Eu-152	48.69 μCi	49.5	43.03 +/- 0.14 μCi
Eu-152	0.55 μCi	5	0.733 +/- 0.003 μCi

In the above table, GADRAS-DRF estimates the activity most accurately when the measurement is taken at the same distance that the characterization is generated for. GADRAS-DRF can analyze sources at various distances, but it extrapolates the response and so the further you get from the characterization distance, the more GADRAS-DRF needs to extrapolate. A comprehensive study on the extrapolation with various detectors and in different environments was done previously [5].

3.4.2. M400 DRF at 5cm

At close distances, GADRAS-DRF computes and accounts for true-coincidence summing (TCS) so there is no need to correct for counts lost in peaks due to TCS. An example spectrum of Co-60 with TCS present is shown below in Figure 27.

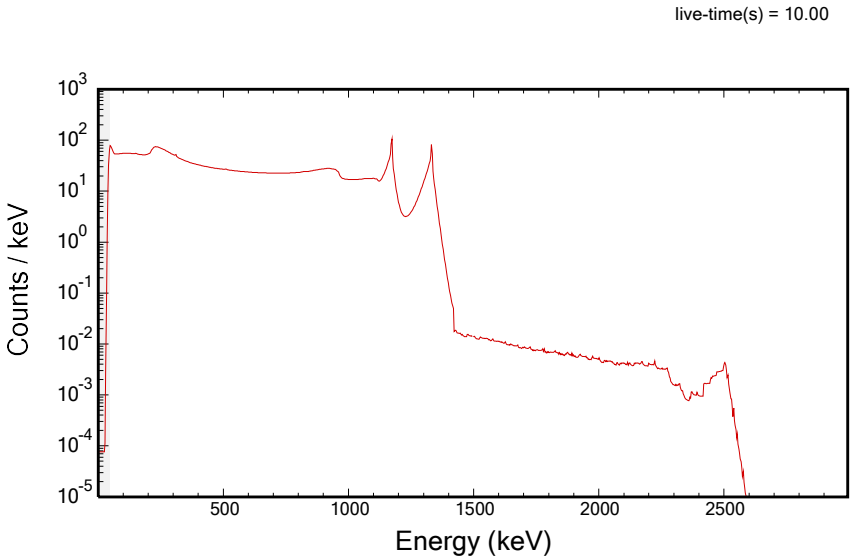

Figure 27. Computed Co-60 spectrum in GADRAS-DRF that is close enough to the detector to exhibit TCS.

The main inaccuracies that come from close source to detector calculations in GADRAS-DRF come from the fact that GADRAS-DRF was made for scenarios where the source is around 100 cm away from the detector. For example, GADRAS-DRF makes certain assumptions about the crystal shape and assumes it is always a cylinder, which is a valid assumption for most scenarios, but can lead to inaccurate solutions when the source is 5 cm from the detector – namely path lengths. Further GADRAS-DRF development is needed for the best solution possible in these situations.

The activities of the sources in Table 12 are again the source activities on the measurement date along with the source height and distance. Weaker sources were chosen to minimize detector dead time. The height represents both the center of the detector and source. Photos of the characterization setup can be found below in Figure 28. The characterization results using the sources in the below table are all shown in Figure 25. The DRF is not as accurate for the 5 cm characterization as it is for the 25 cm characterization for the reasons described previously.

Table 12. Sources used for calibration measurements for generating a DRF at 5 cm.

Source	Activity (μC)	Distance (cm)	Height (cm)	Date
Am-241	20.14	5	101.8	04/01/2025
Co-60	2.62	5	101.8	04/01/2025
Ba-133	1.39	5	101.8	04/01/2025
Cs-137	12.98	5	101.8	04/01/2025
U-232	9.58	5	101.8	04/01/2025

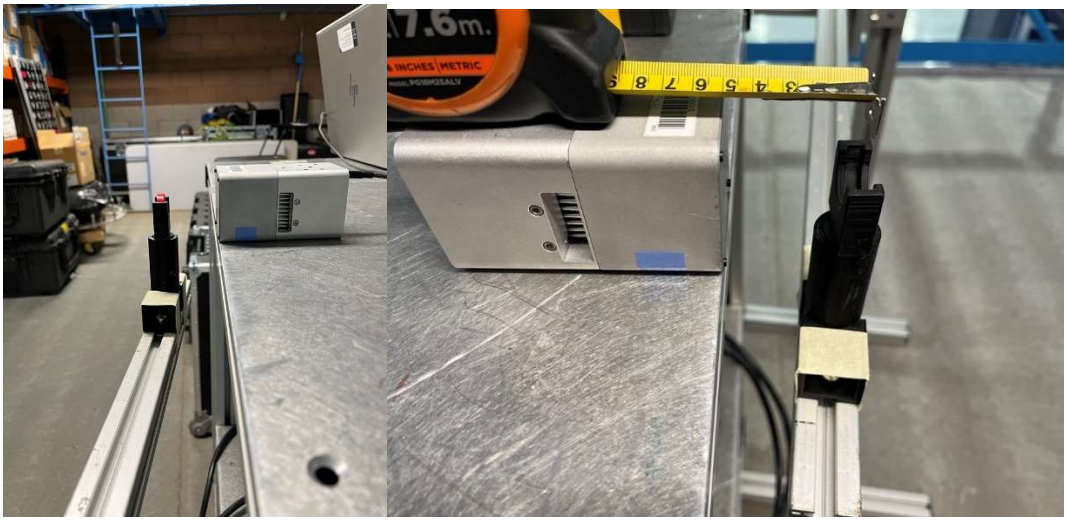

Figure 28. Characterization measurement setup at 5 cm.

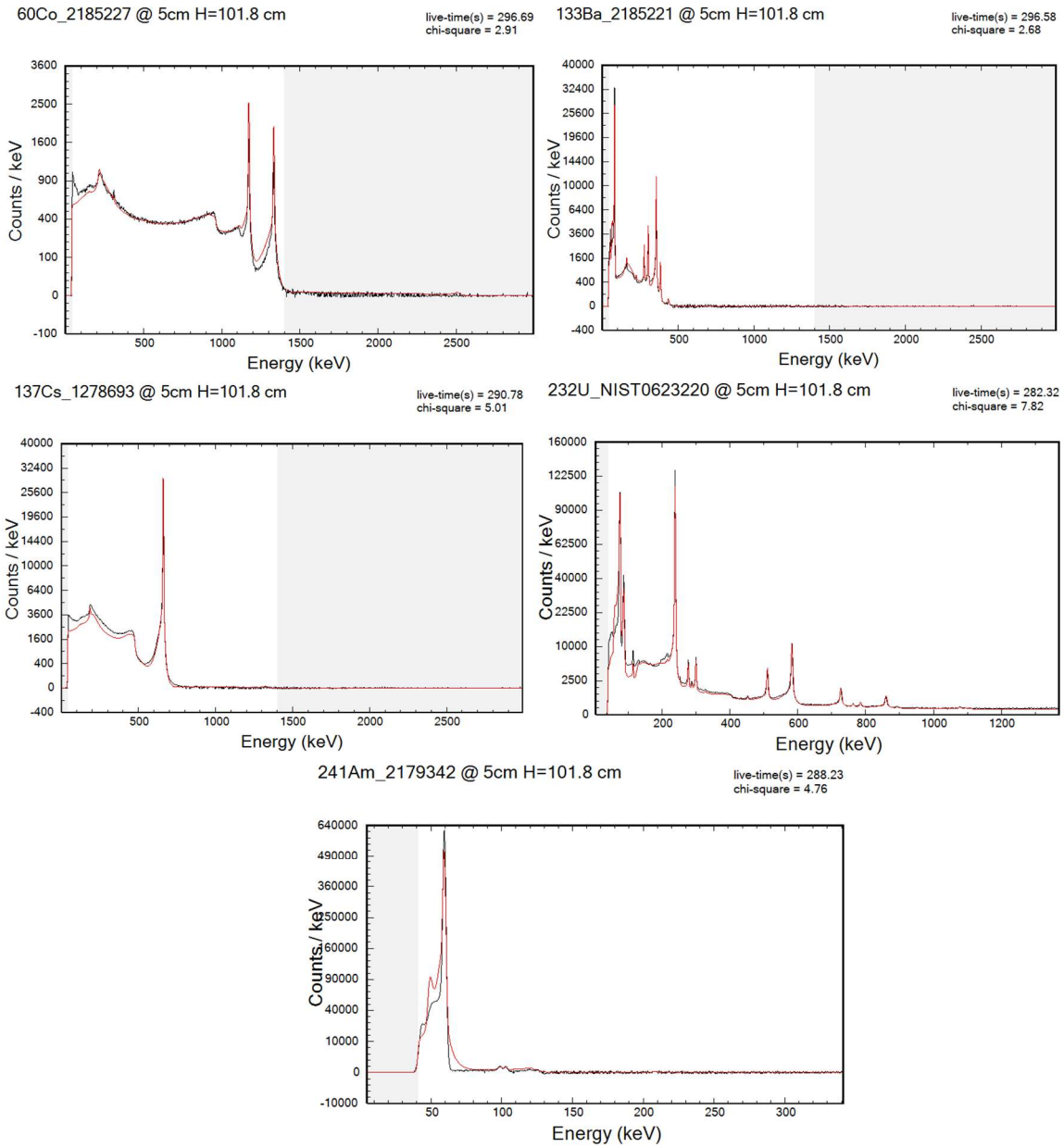

Figure 29. Characterization of the M400 DRF at 5 cm for sources listed. The simulated spectra are red, and the measured spectra are black.

The results are shown in Table 13 below. The Eu-152 estimate at 5 cm is more accurate than in Table 11 since the detector is characterized at that distance and becomes less accurate the further you get from the characterization distance as discussed previously. This is expected because GADRAS-DRF is extrapolating the detector response. It is best practice to take the characterization measurements midway between the range you expect to use the detector.

Table 13. Eu-152 distances, ground truth activity, and estimated activity.

Source	Activity	Distance (cm)	Estimated Activity
Eu-152	48.69 μCi	25	45.47 +/- 0.11 μCi
Eu-152	48.69 μCi	49.5	36.42 +/- 0.11 μCi
Eu-152	0.55 μCi	5	0.639 +/- 0.002 μCi

3.4.3. HPGe Rotating Drum

The same measurements discussed in Section 3.2.1 are used here to look at activity estimates for a non-ideal scenario. For the activity estimates, only the fiberboard drum is analyzed. This measurement is not sufficient for decent quantitative analysis due to the assumptions about the measurement. This statement also applies to the rotating drum measurements using the M400 in the following section. The assumption for this experiment was that a long dwell time measurement with line sources in a rotating drum would approximately resemble a uniformly distributed source all throughout the drum. Other sources of uncertainty are the material compositions of the line source housing, which are metal rods. Since the thickness and geometry of the source are unknown, the accuracy of the activity estimates may suffer, especially for sources that emit lower energy photons.

Two methods were used to obtain activity estimates: one is multiple regression, and the other one utilizes the peak-only model fitting capability in GADRAS-DRF. Multiple regression assumes a point source when the templates are created so it is not generally recommended to use this method when a point source assumption is not valid. The results are shown below in Table 14. The ground truth activities were decayed to the measurement date of 05/11/2021 using the certified activities in Table 1. The Am-241 estimate in the table is likely low because regression assumes that the source is a point source. Whereas, in reality, the Am241 is placed in various locations within the drum and is shielded by varying amounts of fiberboard. Therefore, when a model is used, shielding from further within the drum will be accounted for and the activity estimates will be higher. The areal density specified for multiple regression was bound based on an estimate that the drum is entirely filled with fiberboard and no holes. The settings for regression are shown in Figure 30. The resulting simulated spectrum versus the measured spectrum can also be found in Figure 31 below. In this figure the continuum in the low energy region is not as high as it should be, which indicates that not enough shielding is present in the regression results.

Table 14. Multiple regression result for the fiberboard rotating drum measured with an HPGe.

Source	Activity	Distance (cm)	Estimated Activity
Eu-152	15.93 μCi	100	12.4 +/- 0.06 μCi
Am-241	63.69 μCi	100	11.0 +/- 0.30 μCi
Cs-137	23.20 μCi	100	21.0 +/- 0.12 μCi

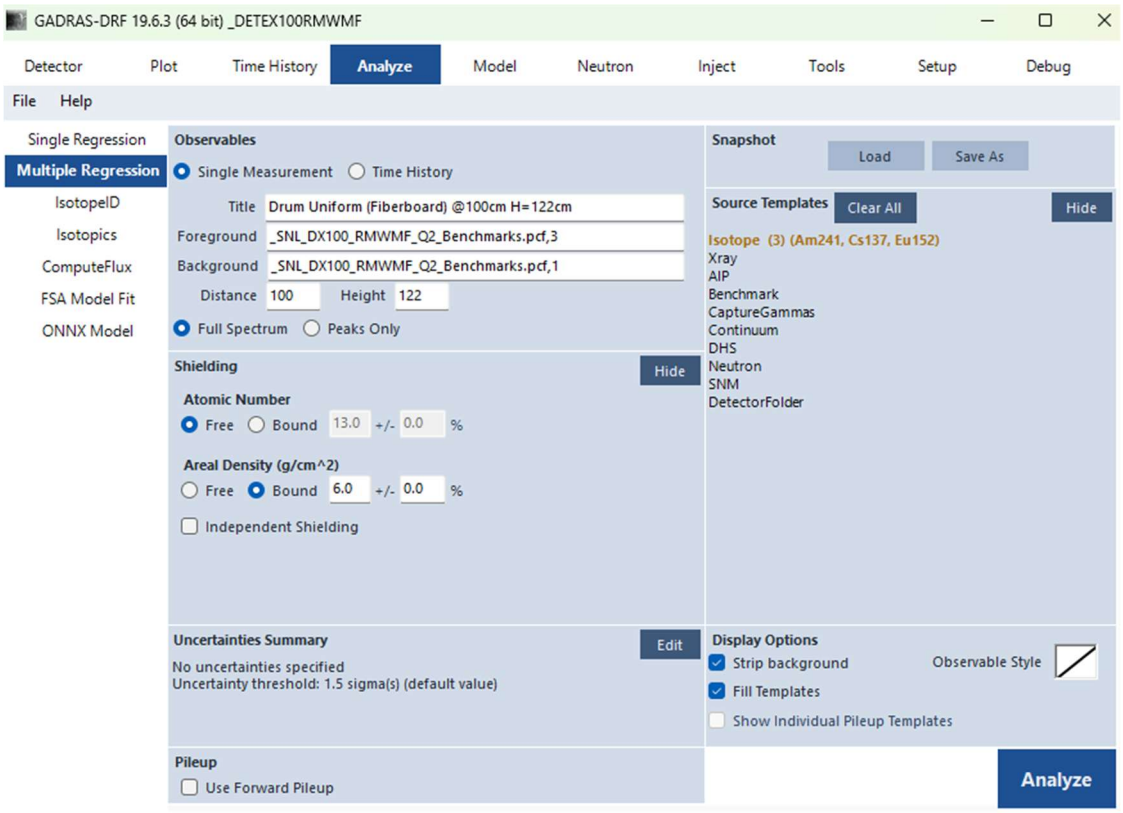

Figure 30. Multiple regression settings for activity estimation of the fiberboard rotating drum measured using an HPGe.

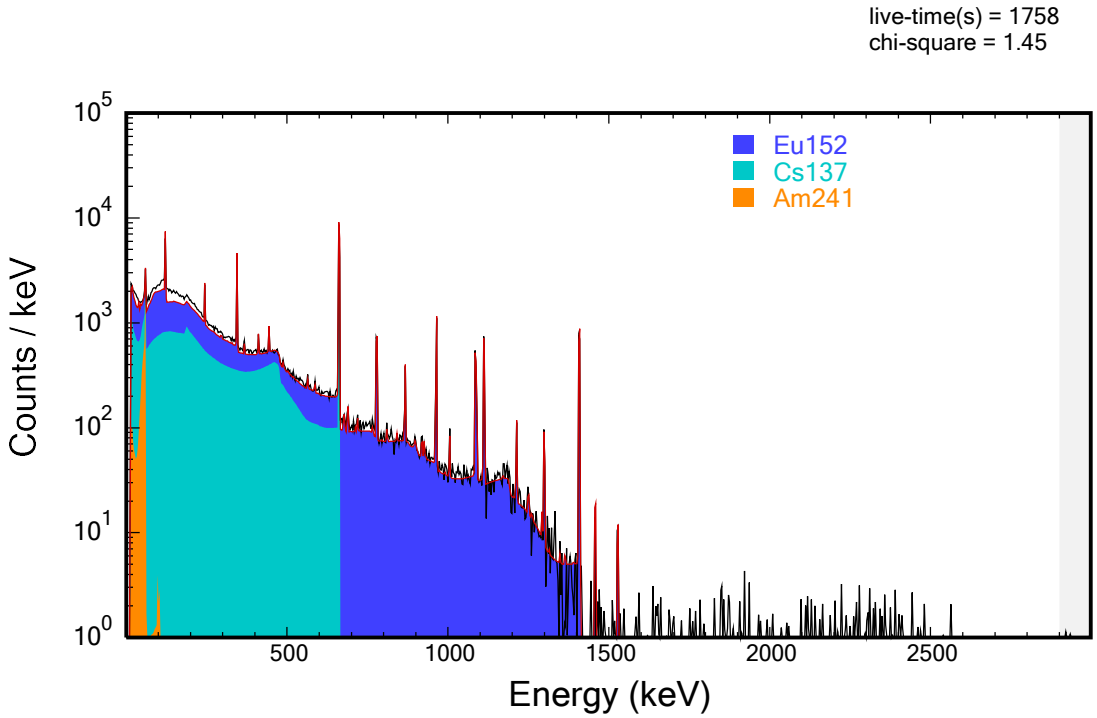

Figure 31. Spectral decomposition of the measured spectrum from the HPGe detector (black).

A very simple drum model was made using the actual drum dimensions. The model consists of two layers in GADRAS-DRF with one layer being the fiberboard with a density of 0.39 g/cc and the other layer is iron with an estimated density of 7.87 g/cc. The source is specified as an evenly distributed source throughout the fiberboard drum. A 3D view of the model is shown below in Figure 32. The results of model fit are shown below in Table 15.

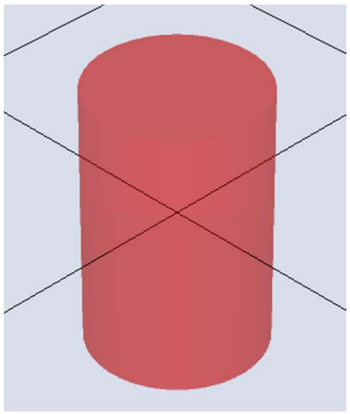

Figure 32. Simple rotating drum model in GADRAS.

Table 15. Model fit results for the HPGe measurement of the rotating drum.

Source	Activity	Distance (cm)	Estimated Activity
Eu-152	15.93 μCi	100	14.8 +/- 1.3 μCi
Am-241	63.69 μCi	100	42.2 +/- 9.2 μCi
Cs-137	23.20 μCi	100	23.9 +/- 2.7 μCi

In the above table, Am-241 is difficult to fit accurately due to the assumption that the source is evenly distributed within the drum. This would mean that most of the Am-241 signal comes from the source that is distributed along the outer edge of the drum due to attenuation of the 59 keV peak. However, the reality is that the linear rods were placed at unknown depths within the drum. If this were modeled exactly along with the thickness of the metal source casing, then the predicted Am-241 would likely be accurate. In the model above, the thickness/material of the metal source casing is also not modeled. The complex shielding scenario results in a complex scenario for estimating the activity of sources that emit low energy photons. The effect is seen much less with the nuclides emitting higher energy photons such as the Eu-152 and the Cs-137. The results in the above table were obtained by using FSA model fit that optimizes the source activities distributed throughout the model of the drum shown in Figure 32. The model fit to the spectrum is shown in Figure 33.

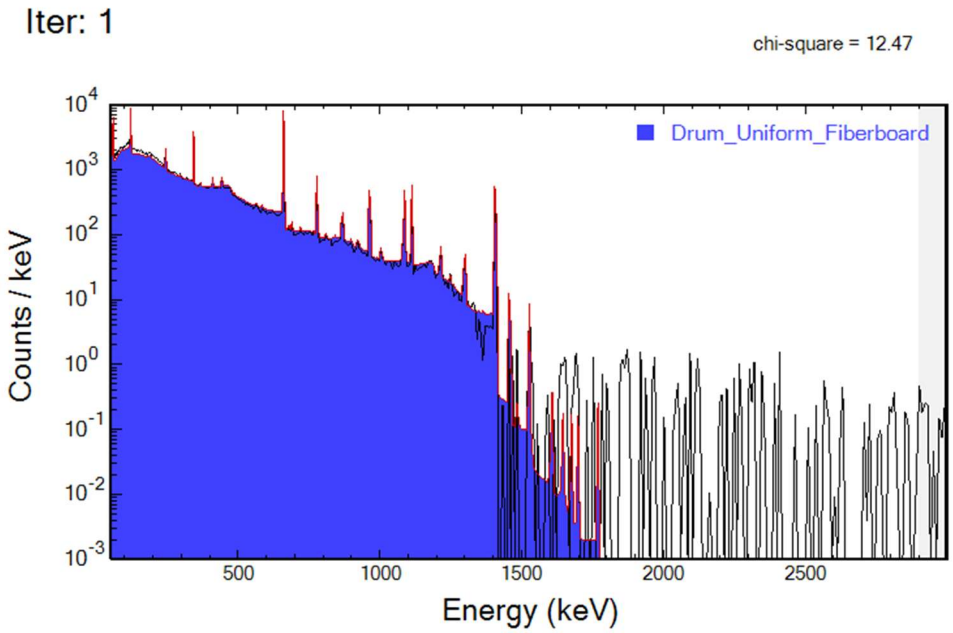

Figure 33. Computed model spectrum in GADRAS compared to the provided measured spectrum.

The same analysis was done using peak only model fit. The result is shown below in Table 16 and the peaks used are shown in Figure 34. The continuum above in Figure 33 is more accurate than Figure 31 because now the scattering within the drum can be more accurately modeled. Scattering is accounted for within the point model, but the point model (multiple regression) assumes a single material. The peak only model fit gave similar activity estimates as the full spectrum model fit.

Table 16. Peak only model fit results for HPGe measurements.

Source	Activity	Distance (cm)	Estimated Activity
Eu-152	15.93 μCi	100	14.0 +/- 1.0 μCi
Am-241	63.69 μCi	100	41.6 +/- 7.7 μCi
Cs-137	23.20 μCi	100	21.2 +/- 3.5 μCi

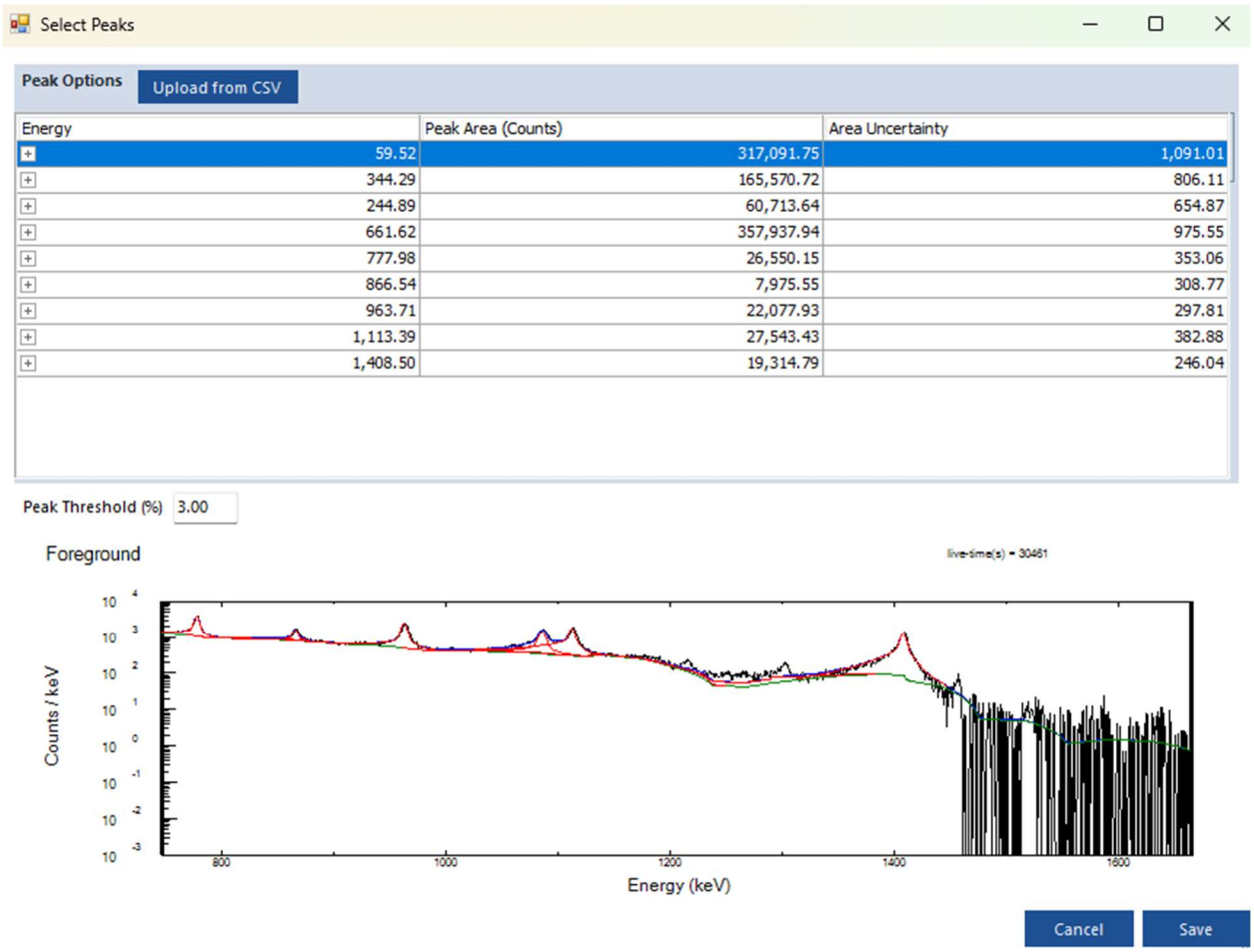

Figure 34. Peak selection form for peak only model fit.

3.4.4. M400 Rotating Drum

The measurements were taken on 6/18/2025 so the ground truth established in the table below is calculated using the certified source activity and in Table 1. The activities of each isotope in each rod were then summed together. GADRAS-DRF was again used to obtain the estimated activities. The diameter of the drum is 59.6 cm so the distance in GADRAS-DRF from the center of the drum to the detector is 53.45 cm with the detector being 25 cm away from the skin of the drum. However, in the table below the distance to the skin is listed. Two different results were used again to obtain activity estimates. The first table below shows the results for multiple regression, which assumes a point source. The areal density was bound based on an estimate that the drum is entirely filled with fiberboard and no holes. The atomic number was allowed to vary as shown in Figure 35 and the spectral decomposition is shown in Figure 36 below. In this figure, it is shown that the continuum is under-estimated. This is likely because a point source is assumed for multiple regression so the scattering within the drum itself is not modeled.

Table 17. Multiple regression results for the fiberboard rotating drum measurement using the H3D M400.

Source	Activity	Distance (cm)	Estimated Activity
Eu-152	12.91 µCi	25	12.6 +/- 0.04 µCi
Am-241	61.97 µCi	25	10.6 +/- 0.20 µCi
Cs-137	21.11 µCi	25	22.3 +/- 0.12 µCi

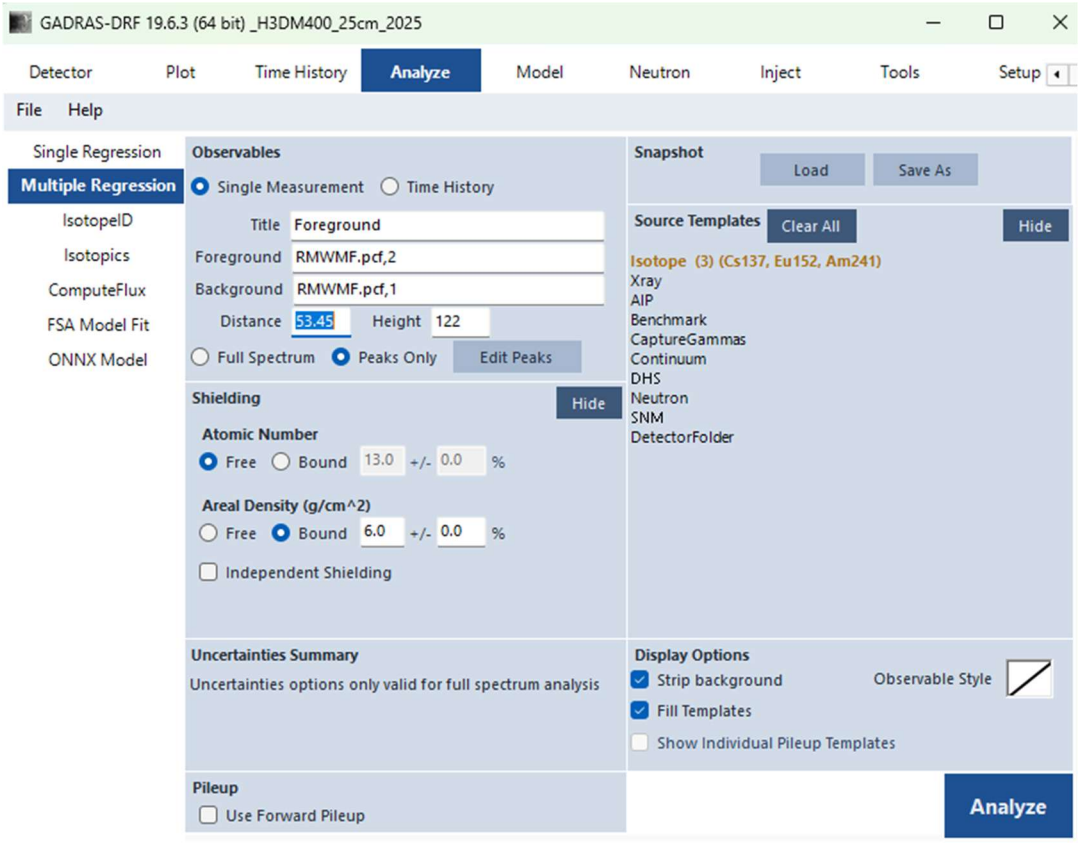

Figure 35. Multiple regression settings for the fiberboard rotating drum measurement.

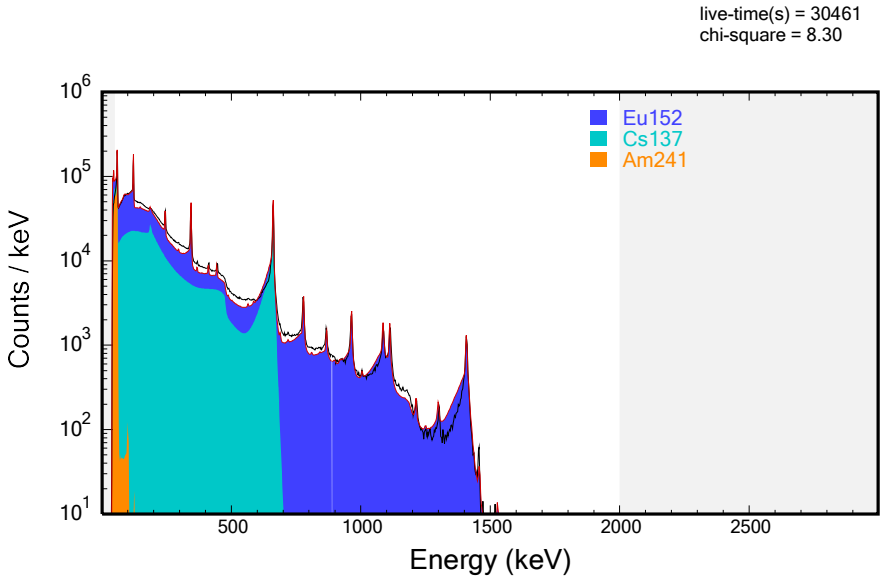

Figure 36. Spectral decomposition of the measured spectrum from the M400 detector (black).

The results in the above table from multiple regression follow the same trend as it did for the HPGe detector. As before with the HPGe, FSA model fit and peak only model fit analysis methods were used to estimate the activities. The same uniform drum filled with fiberboard in Figure 32 was used. The FSA model fit results are below in Table 18, and the fit to the spectrum is shown in Figure 37. Compared to Figure 36, the continuum in Figure 37 is a better fit due to the model used as now scattering is more accurately accounted for since the multiple regression routine assumes only one material for scattering.

Table 18. Model fit results for the M400 measurement of the rotating drum.

Source	Activity	Distance (cm)	Estimated Activity
Eu-152	12.91 μCi	25	15.3 +/- 0.8 μCi
Am-241	61.97 μCi	25	48.8 +/- 8.0 μCi
Cs-137	21.11 μCi	25	27.8 +/- 1.3 μCi

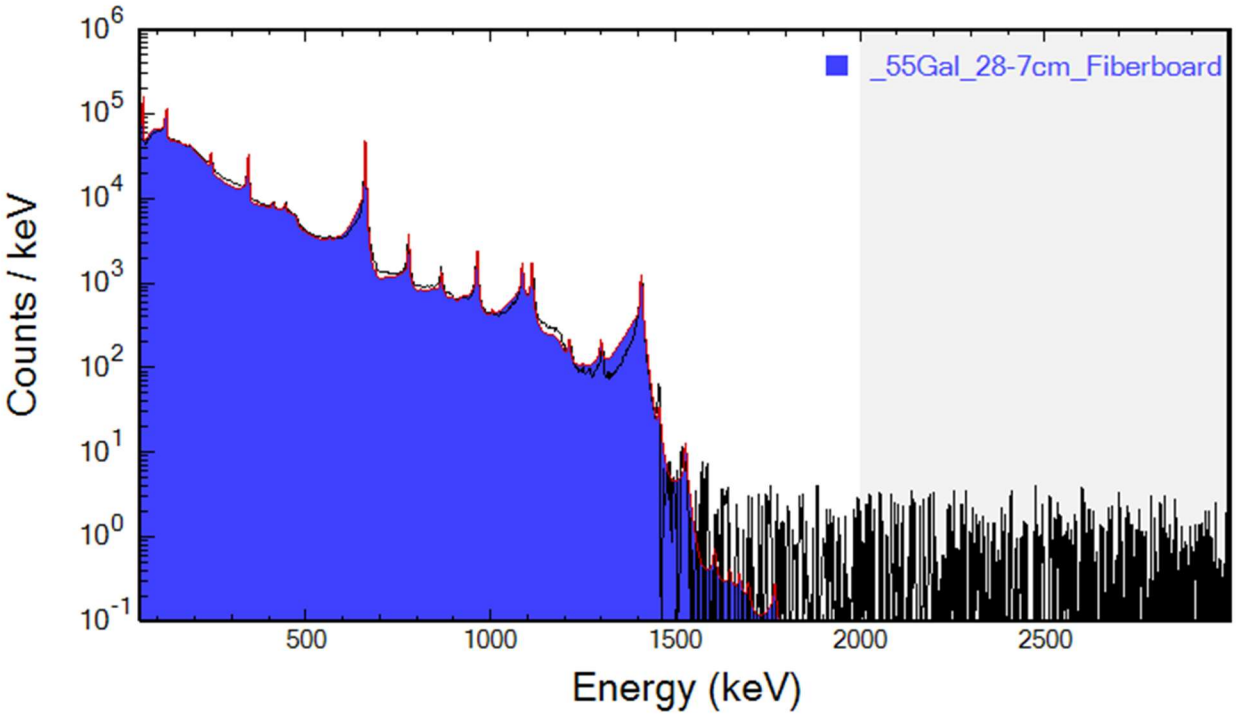

Figure 37. Computed model spectrum in GADRAS compared to the provided measured spectrum.

As expected, the Am-241 is again underestimated. Peak only model fit was also used and those results are below. The same peaks as in Figure 34 were used in the analysis. Due to the shape of the M400 photopeaks, it is more difficult to estimate the activity based on the peaks and the uncertainty on the estimates is much higher.

Table 19. Peak only model fit results for the M400 measurement of the rotating drum.

Source	Activity	Distance (cm)	Estimated Activity
Eu-152	12.91 μCi	25	9.7 +/- 1.7 μCi
Am-241	61.97 μCi	25	38.6 +/- 15.7 μCi
Cs-137	21.11 μCi	25	17.3 +/- 7.0 μCi

4. CONCLUSION

In this document, IsotopeID was validated in various scenarios. One was for a uniformly distributed source, and the other was for situations where the measurements were taken at distances different than the characterization measurements. IsotopeID was also validated for NBL standard measurements. In all scenarios, IsotopeID correctly identified the radionuclides present. The isotopics algorithm was also validated using the BeRP ball measurements, and the NBL standards. GADRAS's capability to estimate activities was also analyzed for various measurement distances when the measurements to be analyzed were different than the characterization measurements. As expected, the activity estimates are most accurate when the measurements are at the same distance that the detector was characterized at, and became less accurate the further the measurement was from the characterization distance. Improvements can be made to GADRAS-DRF for the 5 cm distances. This is because GADRAS-DRF was made for further distance scenarios, so some assumptions are made about the crystal geometry. Further development is needed to model such near field measurements more accurately. This kind of development would include adding more scattering parameters for characterization on the detector page. It was also demonstrated that GADRAS-DRF accounts for TCS in close source to detector geometries.

The M400 was used to take measurements of a rotating drum in an attempt to simulate a uniformly distributed source. These measurements were used for the IsotopeID validation described above. These measurements, along with ones previously taken with a Detective-EX100, were used to obtain the activity estimates using the following algorithms in GADRAS-DRF: multiple regression, FSA model fit, and peak only model fit. For all methods, the activities for Cs-137 and Eu-152 resulted in decent activity estimates. There were unknowns about the line sources that could not be modeled that shielded the Am-241 59 keV peak. Overall, it would be better to obtain measurements of actual uniformly distributed sources. Lastly, fixes such as the uncertainty estimates for plutonium isotopics will be made to GADRAS-DRF before the next release.

REFERENCES

[1] S.M. Horne, et. al., "GADRAS-DRF Version 18 User's Manual", Sandia National Laboratories, SAND2019-14655, December 2019.

[2] D.J. Mitchell et. al, "GADRAS Detector Response Function" Sandia National Laboratories SAND2014-19465, November 2014.

[3] M. R. Smith, et al, "GADRAS-DRF Enhancements for Safeguards", Sandia National Laboratories SAND2023-09056O, September 2023.

[4] M. R. Smith, et al, "GADRAS-DRF Enhancements for Safeguards – Custom Peak Fitting to Enhance Model Fitting and Isotopics", Sandia National Laboratories SAND2024-12182, September 2024.

[5] M. R. Smith, et al, "Quantifying Extrapolation Accuracies of GADRAS-DRF Response Functions", Sandia National Laboratories SAND2023-09073O, September 2023.

[6] J.K. Mattingly and D.J. Mitchell, *A Framework for the Solution of Inverse Radiation Transport Problems*, IEEE Trans. Nucl. Sci, vol. 57, no. 6 2010.

[7] *H3D M Series Detector*, H3D, https://h3dgamma.com/m400.php.

[8] S.D. Rasberry, "Standard Reference Material 969, Uranium Isotopic Standard Reference Material for Gamma Spectrometry Measurements", Office of Standard Reference Materials, June 1985.

[9] M.E. Tolbert, "CRM 146, Uranium Isotopic Standard For Gamma Spectrometry Measurements", New Brunswick Laboratory, July 1999.

[10] Michael W. Enghauser, et. al., "Gamma spectrometry uranium isotopic analysis rodeo: Summary of GADRAS results", Sandia National Laboratories, SAND2021-12417 R, September 2021.

[11] S. Walston, et. al., "Benchmark Measurements of the BeRP Ball in Various Reflectors", Lawrence Livermore National Laboratories, LLNL-TR-661297, September 24 2014.

DISTRIBUTION

Email—Internal

Name	Org.	Sandia Email Address
Heidi Smartt	06817	hasmart@sandia.gov
Technical Library	1911	sanddocs@sandia.gov

Email—External

Name	Company Email Address	Company Name
Nina Rodriguez	nina.rodriguez@nnsa.doe.gov	NNSA
Ramkumar Venkataraman	ramkumar.venkataraman@nnsa.doe.gov	NNSA

This page left blank

Sandia National Laboratories

Sandia National Laboratories is a multimission laboratory managed and operated by National Technology & Engineering Solutions of Sandia LLC, a wholly owned subsidiary of Honeywell International Inc. for the U.S. Department of Energy's National Nuclear Security Administration under contract DE-NA0003525.